

Dirac Representation for Lattice Spin Operators: Spin-1/2 and Spin-1 cases

Maseim B. Kenmoe¹

¹*Mesoscopic and Multilayer Structures Laboratory, Faculty of Science,
Department of Physics, University of Dschang, Cameroon*

(Dated: April 17, 2025)

A novel quantum representation of lattice spin operators (LSOs) is achieved by mapping quantum spins onto their classical analogues for spin size $S = 1/2$ and $S = 1$. The “braket” representations of LSOs are attained thanks to a profound inspection into the binary/ternary distribution of classical bits/trits in non-negative integers. We claim the possibility of getting the j th digit of a positive integer without performing any binary/ternary decomposition. Analytical formulas returning the j th bits/trits of an integer are presented. Impacts of our achievements in Physics are highlighted by revisiting the 1D spin-1/2 XXZ Heisenberg model with open boundaries in a magnetic field in both absence (uniform magnetic field) and presence of disorder (random magnetic field). In the absence of disorder (clean system), we demonstrate that the corresponding eigenvalues problem can be reduced to a tight-binding problem on a graph and solved without resorting to any spinless transformation nor the Bethe Anzath. In the presence of disorder, a convergent perturbation theory is elaborated. Our analytical results are compared with data from exact diagonalization for relatively large spin systems ($K \leq 18$ spins with K denoting the total number of spins) obtained by implementing both the global $U(1)$ symmetry to block-diagonalize the Hamiltonian and the spin-inversion symmetry for two-fold block-diagonalization in the sector with total magnetization $\mathcal{J}^z = 0$. We observe a good agreement between both results.

I. INTRODUCTION

Dirac once wrote[1]: “A good notation can be of great value in helping the development of a theory”. In quantum Many-Body (MB) theory for spin systems and statistical physics, depending on the problem, it is highly desired to achieve appropriate representation of lattice spin operators (LSOs). These fields rapidly grew during the early periods of quantum mechanics thanks to the efforts due in historical order to Jordan and Wigner (JW)[2], Holstein and Primakoff (HP)[3], J. Schwinger (JS) [4] and Dyson and Maleev(DM)[5, 6], among others. LSOs at the same site span the $SU(2)$ group exhibiting unique features: they commute at different sites and anti-commute at the same site and for these reasons do not admit neither Fermi nor Boson statistics[7, 8]. Despite this difficulty, the above authors succeeded in mapping LSOs onto fermions (in the case of JW) and bosons (in the case of HP, JS and DM). These serve till date as main ingredients in cooking up quantum theories for spin systems, including spin-wave theories[9–11]. They have led to hallmark step-forward in understanding spin systems with various applications.

Inspite an incommensurable list of successes attributed to the aforementioned pioneering works, each of the representations come with certain drawbacks that severely limits its range of applications. Among other things can be listed challenges arising due to dimensionality, non-locality, spin-size, population occupancy, non-linearity, non-Hermiticity and/or temperature dependence. For instance, JW transformations are well-suited for 1D systems as in higher dimension it induces non-locality[12] in the form of string operators. HP transformations are advantageous for

large spin-size systems and are adapted for higher dimension as they preserve locality. However, they require truncation/approximation of square root leading to non-linearity and are consequently not convenient for spin-1/2 due to poor convergence of the approximations. The DM transformation exhibits non-Hermiticity, yet it remains preferable to the Holstein-Primakoff transformation –not only due to its simplicity in spin-wave theory but primarily because non-Hermitian effects are negligible. Several alternative representations were developed to cure these limitations among which include, the pseudofermions Abrikosov[13], Popov-Fedotov semionic[14, 15] and Majorana representations[16–18]. Yet, like the previously mentioned transformations these ones also come with severe constraints. No universal representation that copes with the entire spectrum of unsolved problems in Condensed Matter Physics and related fields has so far been invented.

We propose viable Dirac (bra-ket) representations for 1D spin-1/2 and spin-1 LSOs free from any non-locality, non-linearity and non-Hermiticity. We realize a quantum-to-classical correspondence by writing LSOs in a classical basis (binary and ternary bases) while preserving their quantum nature. This became possible by mapping qubits/qutrits onto their classical analogue, the classical bits/trits. Similar tasks are accomplished in Refs.[19–21] for numerical treatment of coordinates and momentum on one hand, energy and time on the other hand. LSOs representation remaining of valuable importance. Dirac notations are typically desired because of their inherent abstract algebra that alleviates manipulation of the associated observables. They could hold the promise to be useful in the MB theory to decipher the non-trivial mechanism behind quantum phe-

nomenon such as quantum entanglement[22, 23], topological phase of matter[24], spin liquids and MB localization (MBL)[25, 26] just to list a few. They pave a way for further insight into the spin-wave theory. For example, in Ref.[27] such a notation is achieved for the LSO in the quantization direction in terms of the floor function and used to identify the complete set of integrals/constants of motion claimed as potential candidates for describing MBL.

In the ongoing discussion, the derived Dirac representations are employed to revisit the eigenspectrum of the 1D spin-1/2 XXZ Heisenberg model incorporating anisotropy in an open boundary configuration without resorting to the Bethe anzath. An additional Ising term is included, involving local magnetic fields h_j with j indexing lattice sites. The model has global $U(1)$ symmetry allowing treatments in sectors corresponding to fixed magnetization quantum number. In the sector with zero magnetization, spin-inversion symmetry is invoked allowing to break down the Hamiltonian into yet two disconnected sectors corresponding to the eigenvalues of the spin-inversion operator. Two complementary limits of the magnetic field are considered: (i) the uniform and non-uniform magnetic fields. For uniform local magnetic fields ($h_j = h$, clean models), the eigenvalue equations are reduced to tight-binding equations and solved exactly in each sector. In the case of non-uniform local magnetic fields (all h_j different e.g. disordered or contaminated models), the eigenspectra are derived using a perturbation theory with respect to the spin-spin exchange J . Our results are compared with data from exact diagonalization obtained by invoking the aforementioned symmetries for relatively large-size spin systems and validated in both the antiferromagnetic ($J < 0$) and ferromagnetic exchange regimes ($J > 0$). An excellent agreement between both data is observed when the perturbation parameter satisfies the condition $|J| \leq 1$.

The remaining part of the paper consists of 5 + 1 Sections structured as follows: Section II aims at clarifying the position of the problem addressed in this piece of paper. We demonstrate that the state-of-art of our current knowledge on LSOs permits Dirac notations that only hold for few-body problems becoming cumbersome when more particles are added. Thence, the need to invent a more convenient representation. The novel representation is presented for spin-1/2. Section III is devoted to demonstrating that a well-defined problem can easily be solved. The impact of our representations in the Physics of integrable models including the 1D Heisenberg model is highlighted. A non-integrable version is discussed in Section IV. The representation for spin-1 is elaborated in Section V but applications are deferred to future projects. Section VI concludes the paper and a few Appendices are provided as additional materials for deeper understanding of our main results.

II. QUANTUM-TO-CLASSICAL MAPPING

A. Quantum Representation

Consider a chain of K identical spins of size S . Each spin lives in a local Hilbert space $\mathcal{H}^{(j)}$ (with $j = 1, \dots, K$) spanned by the basis vectors $|m_S^{(j)}\rangle$ (with $-S \leq m_S^{(j)} \leq S$, the eigenvalues of spin vectors along the quantization direction). The composite Hilbert space necessary to capture the dynamics of the ensemble expresses as the tensor-product of local sub-spaces,

$$\mathcal{H} = \bigotimes_{j=1}^K \mathcal{H}^{(j)}. \quad (2.1)$$

This space is of dimension $D = d^K$ with $d = 2S + 1$ and spanned by the basis vectors,

$$|m_S^{(1)} \dots m_S^{(j)} \dots m_S^{(K)}\rangle \equiv \otimes_{j=1}^K |m_S^{(j)}\rangle. \quad (2.2)$$

These vectors are mutually orthogonal with a unique completeness relation thus forming a complete set of vectors. Denoting as $\hat{\vec{S}}_j = [\hat{S}_j^x, \hat{S}_j^y, \hat{S}_j^z]$ the spin vector acting on the local subspace $\mathcal{H}^{(j)}$ and introducing the corresponding ladder operators $\hat{S}_j^\pm = \hat{S}_j^x \pm i\hat{S}_j^y$ (seen to be non-Hermitian), then the spin action at an indicated site is evaluated through ($\hbar = 1$)

$$\hat{S}_j^\pm |m_S\rangle_j = \lambda_{\pm m_S^{(j)}} |m_S^{(j)} \pm 1\rangle_j, \quad (2.3)$$

$$\hat{S}_j^z |m_S\rangle_j = m_S^{(j)} |m_S^{(j)}\rangle_j, \quad (2.4)$$

with $\lambda_{\pm m_S^{(j)}} = [S(S+1) - m_S^{(j)}(m_S^{(j)} \pm 1)]^{1/2}$ as found in many textbooks of quantum mechanics (see for e.g. Ref.[28]). In the above relations $|m_S\rangle_j$ is a shorthand notation for the basis vector in Eq.(2.2). The extra subscript is usually inserted to put an accent emphasis on the considered lattice site. One easily observes that the action of the lattice ladder spin operators \hat{S}_j^\pm onto a given configuration increases/decreases the j th quantum number by a unit. We shall see in our representation that this remark is rather counter-intuitive (see Section II B).

Although the above relations at first glance look simple and elegant as one might expect the action of quantum operators to be, the intrinsic reality is rather complex. Indeed, a concrete Dirac (“bra” and “ket”) representation inferred from Eqs.(2.3) and (2.4) reads

$$\begin{aligned} \hat{S}_j^\pm &= \sum_{m_S^{(1)}=-S}^S \dots \sum_{m_S^{(j)}=-S}^S \dots \sum_{m_S^{(K)}=-S}^S \lambda_{\pm m_S^{(j)}} \\ &\times |m_S^{(1)} \dots m_S^{(j)} \pm 1 \dots m_S^{(K)}\rangle \langle m_S^{(K)} \dots m_S^{(j)} \dots m_S^{(1)}|, \end{aligned} \quad (2.5)$$

$$\hat{S}_j^z = \sum_{m_S^{(1)}=-S}^S \cdots \sum_{m_S^{(j)}=-S}^S \cdots \sum_{m_S^{(K)}=-S}^S m_S^{(j)} \\ \times |m_S^{(1)} \cdots m_S^{(j)} \cdots m_S^{(K)}\rangle \langle m_S^{(K)} \cdots m_S^{(j)} \cdots m_S^{(1)}|. \quad (2.6)$$

And we see that Eqs.(2.3) and (2.4) concretely involve as many summations as there are spins in the system. They are suitable for analytical treatments of few-body systems as one can manually write down all possible configurations and handle a few summations. This suggests that the full Hilbert space can be constructed. For example, consider a spin-1/2 three-body system. The Hilbert space is spanned by $2^3 = 8$ basis vectors. They can all be manually constructed. Two possible such vectors are $|\frac{1}{2}\frac{1}{2}\frac{1}{2}\rangle$ and $|\frac{-1}{2}\frac{1}{2}\frac{1}{2}\rangle$. A matrix element of an observable \hat{A} is $\langle -\frac{1}{2}\frac{1}{2}\frac{1}{2} | \hat{A} | \frac{1}{2}\frac{1}{2}\frac{1}{2} \rangle$. We already observe from here that for large spin systems similar notations will be cumbersome involving a large number of summands. This is one of the manifestations of the finite-size effect, a drastic drawback occurring as a consequence of the exponential growth of the Hilbert space with the total number of spins K . For numerical analyzes, this effect extensively restricts the number of implementable spins in actual computers ($K \leq 24$ to the best of our knowledge). We shall see in the Dirac representation that this effect is considerably reduced, matrix elements of observables are written in simple forms, relatively large spin systems can be numerically integrated on small computers ($K \leq 18$, RAM 32Gb with Mathematica 7 in our case). Our objective is to show that there exists better alternatives to Eqs.(2.5) and (2.6) easier to handle both analytically and numerically.

B. Binary theory

Before diving into the classical representation, let us elaborate on a binary theory for spin-1/2 systems. To this end, we consider the above example and relabel the basis vectors as $|\frac{1}{2}\frac{1}{2}\frac{1}{2}\rangle \equiv |8\rangle$ and $|\frac{-1}{2}\frac{1}{2}\frac{1}{2}\rangle \equiv |3\rangle$ such that $\langle -\frac{1}{2}\frac{1}{2}\frac{1}{2} | \hat{A} | \frac{1}{2}\frac{1}{2}\frac{1}{2} \rangle \equiv \langle 3 | \hat{A} | 8 \rangle$. This is the binary representation[29]. It is already simpler compared to the classical one. Indeed, qubits are mapped onto their classical counterparts, the classical bits 0 and 1 as $|\frac{-1}{2}\rangle \equiv |\downarrow\rangle \rightarrow |0\rangle$ and $|\frac{1}{2}\rangle \equiv |\uparrow\rangle \rightarrow |1\rangle$ but counter-intuitively with $|0\rangle = [1, 0]^T$ and $|1\rangle = [0, 1]^T$. Thus, $|\frac{1}{2}\frac{1}{2}\frac{1}{2}\rangle = |111\rangle = |8\rangle$, $|\frac{-1}{2}\frac{1}{2}\frac{1}{2}\rangle = |011\rangle = |3\rangle$.

The binary representation is convenient for numerical analysis, exact diagonalization for example. The Hilbert space can easily be constructed by performing binary decomposition of the basis vectors, which in turn facilitates the construction of the Hamiltonian (see [GitHub repository](#)). We prove that this representations is not just good for numerical simulations but also for analytical treatments[30]. They improve on the readability of observables with consequences on their physical interpretations.

We denote as \mathcal{H}_B the binary space analogue to (2.1) and spanned by $\{|n_S\rangle\}_{n_S=0}^{D-1}$ (basis vectors sorted in lexicographical order). This space is isomorphic to \mathcal{H} . Indeed, there exists a linear bijective map (i.e. both injective and surjective) between them. This map is injective i.e. every element in \mathcal{H} has a unique correspondence in \mathcal{H}_B (one-to-one). The map is surjective (onto) i.e. every element in \mathcal{H}_B has a unique image in \mathcal{H} . If we denote as $\sigma_{n_S}^{(j)} = \{0, 1\}$ the j th digit in the binary decomposition of n_S counting from $j = 1$ in the reading/coding direction—from the left to the right then,

$$n_S = \left(\sigma_{n_S}^{(1)} \cdots \sigma_{n_S}^{(j)} \cdots \sigma_{n_S}^{(K)} \right)_2, \quad n_S = \sum_{j=1}^K \left(\sigma_{n_S}^{(j)} \right) q_j, \quad (2.7)$$

with $q_j = 2^{K-j}$ a weight defined such that the largest number is $\sum_{j=1}^K q_j = (2^K - 1)$ (number with all digits equals to 1). For reading/coding direction—from the right to the left $n_S = \sum_{j=1}^K \left(\sigma_{n_S}^{(K+1-j)} \right) r_j$ where $r_j = 2^j$.

In the first relation in (2.7), subscript 2 refers to the base $b_2 = \{0, 1\}$. Representations (2.7) are easier to interpret compared to (2.2) which involves alternating $|1/2\rangle$ and $|-1/2\rangle$ in a non-trivial manner especially for large systems. Indeed, geometrically, if we define the bits-vector $\sigma_{n_S} = [\sigma_{n_S}^{(1)}, \sigma_{n_S}^{(2)}, \dots, \sigma_{n_S}^{(K)}]$ and the weight-vector $q = [q_1, q_2, \dots, q_K]$ (arithmetic basis) we see that $n_S = \sigma_{n_S} \cdot q$ is a weighted sum of $\sigma_{n_S}^{(j)}$ i.e. a scalar product (not in the Euclidean sense). The $\sigma_{n_S}^{(j)}$ being the coefficient of the binary expansion of n_S determine the presence or absence of q_j in the weighted sum.

As indicated in Refs.29 and 31 the binary representation of n_S encapsulates the exact configuration of spins in the state (2.2) provided that one starts from $n_S = 0$, thence the quantum-to-classical mapping $m_S^{(j)} \rightarrow \sigma_{n_S}^{(j)}$. Let us now describe in the frame of this mapping how LSOs act onto the basis vectors of \mathcal{H}_B . When \hat{S}_j^\pm acts upon the state $|n\rangle$ and meets $\sigma_n^{(j)} = 0$ at the j th position, it destroys the state and returns 0. When in contrary it encounters $\sigma_n^{(j)} = 1$, then it returns 1 and flips the corresponding bit leading to a new state. A similar reasoning applied to \hat{S}_j^- yields the expressions[32],

$$\langle m | \hat{S}_j^\pm | n \rangle = s_n^{(j)\pm} \delta_{m, \mu_j^{[n]}}, \quad (2.8a)$$

$$\langle m | \hat{S}_j^z | n \rangle = s_n^{(j)z} \delta_{m, n}, \quad (2.8b)$$

where $\mu_j^{[n]} = \text{flip}(n, j)$ is the integer obtained after flipping the j th digit in the binary representation of n (See Refs.29 and 31). Here, we have defined,

$$s_n^{(j)+} = \frac{1 - \gamma_n^{(j)z}}{2}, \quad s_n^{(j)-} = \frac{1 + \gamma_n^{(j)z}}{2}, \quad s_n^{(j)z} = \frac{\gamma_n^{(j)z}}{2}, \quad (2.9)$$

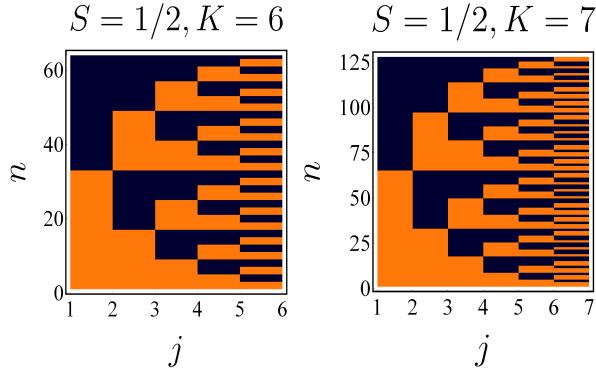


Figure 1. Spin-1/2 distribution for two configurations of bit-field lengths $K = 6$ and $K = 7$. For generating data, we considered integers in $0 \leq n \leq 2^K - 1$ and $1 \leq j \leq K$ and perform binary decomposition. We see that spins along the quantization direction follow a *defined* pattern and are *not* randomly distributed as one may think. As yet another observation, consecutive even and odd numbers only differ by the least significant digits (LSDs). For example 0 (even) and 1 (odd) only differ by LSDs same for 2 (even) and 3 (odd) etc (See Tables II and III). The color palette contains only two colors. Yellow color $\rightarrow -1/2$ and dark-blue $\rightarrow 1/2$ and this explains why it is not depicted.

with $\gamma_n^{(j)z} = 1 - 2\sigma_n^{(j)}$ and $\gamma_n^{(j)z} = \{-1, 1\}$. They correspond to classical bits at site j in the configuration n namely $s_n^{(j)+} \equiv \sigma_n^{(j)}$ and $s_n^{(j)-} = 1 - \sigma_n^{(j)} \equiv \bar{\sigma}_n^{(j)}$. A few of their properties are displayed in Appendix B.

We gain further insight into the `flip()` function by noticing from Eq.(2.7) that as $\bar{\sigma}_n^{(j)}$ denotes the reversed digit of $\sigma_n^{(j)}$ then,

$$\mu_j^{[n]} = n + (\bar{\sigma}_n^{(j)} - \sigma_n^{(j)}) q_j. \quad (2.10)$$

We learn from here that flipping an integer n of bit-field length K at the j th site is equivalent to adding q_j (if $\sigma_n^{(j)} = 0$) or subtracting q_j (if $\sigma_n^{(j)} = 1$) to the said number. For instance, consider the set of non-negative integers of bit-field length $K = 6$ i.e. $0 \leq n \leq 2^6 - 1$. Consider again $n = 5$ in the binary basis, $5 = (000101)_2$. Let us reverse the second digit counting from the left to right i.e. $j = 2$. Because $\sigma_5^{(2)} = 0$ reversing this digit yields $(010101)_2 = 21$ which is nothing but $5 + 2^{6-2} = 21$ ascertaining our assertion. In the same vein, it can be proven that $\mu_j^{[0]} = q_j$ and that $\mu_j^{[D-1]} = D - 1 - q_j$. Similarly, the integer \bar{n} obtained after reversing all digits in an integer n reads, $\bar{n} = n + \sum_{j=1}^K (\bar{\sigma}_n^{(j)} - \sigma_n^{(j)}) q_j = \sum_{j=1}^K \bar{\sigma}_n^{(j)} q_j = D - 1 - n$ whereby, $\sigma_{\bar{n}}^{(j)} = \bar{\sigma}_{\bar{n}}^{(j)}$. For even integers, the least significant digit (LSD) $\sigma_n^{(K)} = 0$, $\mu_K^{[n]} = n + 1$ while for odd integers the LSD is $\sigma_n^{(K)} = 1$ and $\mu_K^{[n]} = n - 1$. Note that the LSD is the digit at $j = K$ as we read from the left to the

right. Eq.(2.10) can now be regarded as

$$\mu_j^{[n]} = \begin{cases} n + q_j, & \text{if } \sigma_n^{(j)} = 0 \\ n - q_j, & \text{if } \sigma_n^{(j)} = 1 \end{cases}, \quad \mu_j^{[\mu_j^{[n]}]} = n. \quad (2.11)$$

Then, n and $\mu_j^{[n]}$ only differ at the j th site where a bit is reversed. Remarkably, as for $\sigma_n^{(j)} = 0$ the integer obtained after flipping this bit is $n + q_j$ we infer that $\sigma_{n+q_j}^{(j)} = 1$. Similarly, as $\sigma_n^{(j)} = 1$ and the bit resulting from inversion is $n - q_j$ then $\sigma_{n-q_j}^{(j)} = 0$. Note also that given an integer q_j (i.e. a number consisting of 0 everywhere excepted the j th position) it can be verified that $\sigma_{q_j}^{(i)} = \delta_{i,j}$.

C. Classical representation

Now, based on Eqs.(2.8a)-(2.8b) and their trivial relations with ladder spin operators and thanks to Eq.(2.11), we can now make manifest the promised Dirac representation for spin-1/2 (See also Ref.27),

$$\hat{S}_j^+ = \sum_{n=0}^{D-1} s_n^{(j)-} |n\rangle \langle n + q_j|, \quad (2.12a)$$

$$\hat{S}_j^- = \sum_{n=0}^{D-1} s_n^{(j)-} |n + q_j\rangle \langle n|, \quad (2.12b)$$

$$\hat{S}_j^z = \sum_{n=0}^{D-1} s_n^{(j)z} |n\rangle \langle n|. \quad (2.12c)$$

As promised, the above representations are simpler than their quantum counterparts. Representation of LSOs in terms of classical variables involve a single summation over the entire Hilbert space \mathcal{H}_B whereas their equivalent quantum counterparts require as enough summations as the number of spins in the chain and this is clearly a major advantage. The finite-size effects arising in the quantum world have considerably been attenuated. It can be verified that our results do not suffer from any non-linearity, non-locality nor non-Hermiticity and are extendable to higher spin-size (See Section V for spin-1). Importantly, they preserve the $su(2)$ algebra. For a single spin system, $K = 1$ i.e. $j = 1$, we retrieve the traditional representation for Pauli matrices σ^α (with $\alpha = x, y, z$)[33], $\hat{S}_1^+ = |0\rangle \langle 1| \equiv \frac{1}{2}\sigma^+$, $\hat{S}_1^- = |1\rangle \langle 0| \equiv \frac{1}{2}\sigma^-$ and $\hat{S}_1^z = \frac{1}{2}(|0\rangle \langle 0| - |1\rangle \langle 1|) \equiv \frac{1}{2}\sigma^z$ where $\sigma^\pm = \sigma^x \pm i\sigma^y$. The above representations can also be regarded as generalization of “braket” representation of Pauli’s matrices for LSOs.

It should be observed that the representation (2.12a)-(2.12c) involves only $s_n^{(j)-}$. This ensures that $(\hat{S}_j^\pm)^\dagger = \hat{S}_j^\mp$ given that the embedded classical objects are Hermitian,

$(s_n^{(j)\pm})^\dagger = s_n^{(j)\pm}$. A second representation in terms of $s_n^{(j)\pm}$ can be achieved[34].

At this stage, it is important to underline that our goal is uncompleted. As already mentioned, $s_n^{(j)\pm}$ is the coefficient of q_j in the binary decomposition of n . This remark suggests from common perception that $s_n^{(j)\pm}$ can only be numerically evaluated (i.e. for large numbers with the aid of a computer and/or manually for small numbers). We have successfully disproved this claim by writing $s_n^{(j)\pm}$ in analytical form such that one can obtain the j th digit of a number without binary decomposition. Indeed, after a profound inspection into the binary structure of a few numbers (see Appendix.A for complete proof), we realized that binary digits enter non-negative integers through a well-defined pattern (see Fig.1). We identified this pattern and came up with

$$s_n^{(j)+} = \sum_{m=0}^{r_{j-1}-1} [u(n - (2m+1)q_j) - u(n - (2m+2)q_j)], \quad (2.13a)$$

$$s_n^{(j)-} = \sum_{m=0}^{r_{j-1}-1} [u(n - 2mq_j) - u(n - (2m+1)q_j)], \quad (2.13b)$$

$$s_n^{(j)z} = \frac{1}{2} \sum_{m=0}^{r_{j-1}} (-1)^m [u(n - mq_j) - u(n - (m+1)q_j)], \quad (2.13c)$$

where $r_j = 2^j$ and

$$u(x) = \begin{cases} 1, & x \geq 0 \\ 0, & x < 0 \end{cases}, \quad (2.14)$$

denoting the unit-step function[35]. This completes our goal. It worth putting a special accent emphasis on the fact that $u(x)$ is **not** the Heaviside step function $\Theta(x)$, in other words $u(0) \neq 1/2$ but as stated $u(0) = 1$ (further clarifications are provided shortly). A simple Mathematica program permits to convince oneself of the truthfulness/accuracy of our results. This is done and added to the following [GitHub repository](#). It was shown in Ref.36 that

$$u(x) = \frac{1}{\pi} \left(\arctan(x-1) + \arctan\left(\frac{2-x}{x}\right) + \frac{3\pi}{4} \right). \quad (2.15)$$

Because Eqs.(2.13a)-(2.13c) allow to obtain any digit of a non-negative integer *without* binary decomposition, these could have several applications not just in physics but broadly in science including cryptography, number theory, computer science and many more. As a consequence in physics this offers the possibility to infer the direction of a spin along the quantization direction in a given configuration. Cryptography aims at manipulating binary digits for securing communication and ensuring that only the intended recipients read the information even if it falls into the hands of unauthorized users. The possibility offered by Eqs.(2.13a)-(2.13c) to

obtain the j th digit of a number n without binary decomposition could lead to the development of new cryptography techniques that are more robust, secure and harder to break. Number theory is devoted to the properties of numbers. This could lead to new insight into the properties of numbers and their relationships with one another. In computer science, these could allow the development of faster algorithm for performing binary operations especially for large numbers.

It can be seen that our transformations preserve the $su(2)$ algebra at the same site. They do not induce any non-locality as in the case of JW transformations nor non-linearity as for HP. They remain local and linear. There is also no constraint related to population occupancy. Let us now clarify what we mean by non-locality and non-linearity. LSOs in the spin representation are local i.e. each operator acts solely on a single site and no coupling to other sites is required. In the case of JW representation, a ladder operator acting at site j reads $\hat{S}_j^+ = c_j^\dagger \prod_{k=1}^{j-1} \exp[i\pi c_k^\dagger c_k]$ where c_k^\dagger and c_k are respectively fermion creation and annihilation operators. The factor $\prod_{k=1}^{j-1} \exp[i\pi c_k^\dagger c_k]$ is a non-local string operator as it involves all fermionic sites from 1 to $j-1$. Non-locality arises as consequence of the fact that the string operator must fulfill the fermionic anti-commutation relations. Non-locality makes it hard to extend JW to higher dimensions. For HP, $\hat{S}_j^+ = \sqrt{2S - a_j^\dagger a_j}$ where S is the spin size, a_j^\dagger and a_j are boson creation and annihilation operators respectively. This representation is local but its usage requires approximating the square root. This is done assuming $S \gg 1$ leading to non-linearity in the boson representation. For spin $S = 1/2$, this leads to poor convergence of the truncation.

A few general remarks are in order. Firstly, because of the constraint $n \geq 0$ our treatments hold for

$$s_n^{(j)\pm} = 0, \quad n < 0. \quad (2.16)$$

Secondly, $s_0^{(j)+} = 0$ ($s_0^{(j)-} = 1$, $s_0^{(j)z} = \frac{1}{2}$) and $s_{D-1}^{(j)+} = 1$ ($s_{D-1}^{(j)-} = 0$, $s_{D-1}^{(j)z} = -\frac{1}{2}$) for arbitrary j and K . In what follows, the spectrum of q_j is assumed to fall into the window $1 \leq q_j \leq 2^{K-1}$. Thus, every value of q_j that lies outside this region is conventionally set to 0 i.e. $q_j = 0$ and,

$$q_0 = q_{K+1} = q_{K+2} = \dots = 0. \quad (2.17)$$

While in the quantum representation, acting \hat{S}_j^\pm onto the spin configuration $|n\rangle$ increases/decreases the quantum number by a unit, in the classical case in contrary, this action counter-intuitively decreases/increases the order of the basis vector in \mathcal{H}_B by q_j . Indeed, it can easily be verified that $\hat{S}_j^\pm |n\rangle = s_n^{(j)\pm} |n \mp q_j\rangle$. Therefore, the action of \hat{S}_j^+ onto the basis vector $|n\rangle$ returns the j th bit in the binary representation of n and shifts it to the $(n - q_j)$ th

position in \mathcal{H}_B while \hat{S}_j^- returns the complementary bit $s_n^{(j)-}$ and shifts the basis vector to the $(n + q_j)$ th position.

We have so far achieved a Dirac representation in terms of unit-step function. This is a discrete notation. It would be interesting to move from the discrete to a continuous representation. We use the Heaviside function $\Theta(x)$. It worth noticing that $u(x)$ coincides with $\Theta(x)$ everywhere on the real axis excepted at the origin (turning point) where $u(0) = 1$ while $\Theta(0) = 1/2$. We can rewrite Eqs.(2.13a)-(2.13c) in terms of $\Theta(x)$ by avoiding every point where the argument of $u(x)$ vanishes. This is done by discriminating between even and odd positive integers. Thus, for even n ,

$$s_n^{(j)z} = \frac{1}{2} \sum_{m=0}^{r_j-1} (-1)^m \left(n_F \left(\mathcal{Q}_{n+1,m}^{(j)} \right) + n_F \left(\mathcal{Q}_{n+1,m+1}^{(j)} \right) \right) + \frac{1}{2} \delta_{j,K}, \quad (2.18)$$

while for odd n ,

$$s_n^{(j)z} = \frac{1}{2} \sum_{m=0}^{r_j-1} (-1)^m \left(n_F \left(\mathcal{Q}_{n,m}^{(j)} \right) + n_F \left(\mathcal{Q}_{n,m+1}^{(j)} \right) \right) - \frac{1}{2} \delta_{j,K}, \quad (2.19)$$

and where we have defined the Fermi-like function[33]

$$n_F(x) \equiv \Theta(x) = \lim_{\lambda \rightarrow \infty} \frac{1}{1 + e^{-\lambda x}}, \quad (2.20)$$

with $\mathcal{Q}_{n,m}^{(j)} = n - mq_j$ interpreted as the remainder of the division n/m and q_j the quotient[37]. $s_n^{(j)+}$ and $s_n^{(j)-}$ are calculated from (B7) as $s_n^{(j)\pm} = \frac{1}{2} \left(1 \mp 2s_n^{(j)z} \right)$. Numerical proofs are available in the [GitHub repository](#). We confirm that the LSD for even integers $s_n^{(K)z} = 1/2$ whereas that for odd integers is $s_n^{(K)z} = -1/2$.

The notation $n_F(x)$ is used in reference to the Fermi-Dirac distribution used in quantum statistic to describe the occupancy of energy states by fermions[38]. By comparison, n plays the role of the energy, mq_j the chemical potential at site j and λ (related to the temperature $\lambda = 1/2k_B T$ where k_B is the Boltzmann constant) determines the sharpness of the distribution. The limit $\lambda \rightarrow \infty$ corresponds to the absolute zero temperature regime in the Fermi distribution and $n_F(x)$ transition into a step-like function. In the Fermi sense, for $n > mq_j$ the state is occupied ($n_F = 1$), for $n < mq_j$ the state is empty ($n_F = 0$) and for $n = mq_j$ the state is half-occupied ($n_F = 1/2$). Quantum spins do not possess Fermi distribution while classical spins apparently do.

D. States representation

As already indicated $|n + q_j\rangle$ is the state obtained by flipping the j th bit in the binary representation of $|n\rangle$

provided $s_n^{(j)-} = 0$. Therefore $|n + mq_j\rangle$ could be viewed as the state achieved by flipping the j th bit m times. If m is even, then $|n + mq_j\rangle = |n\rangle$ i.e. the action of flipping a single digit an even number of times takes it back to its initial position preserving the original state. If in opposition m is odd, thus $|n + mq_j\rangle = |n + q_j\rangle$. As a consequence of these observations, every basis vector can be constructed from $|0\rangle \equiv |000 \cdots 000\rangle$ (vacuum state) by inverting local spin directions only once as it is done in quantum mechanics by operational application. Thus,

$$|q_j\rangle = |000 \cdots 1_j \cdots 000\rangle, \quad (2.21)$$

describes all states with one spin in up-state ($K_\uparrow = 1$) the collection of which belongs to the sector with magnetization $\mathcal{J}^z = K_\uparrow/2$ (for even number of spins) provided the Hamiltonian possesses a global $U(1)$ symmetry thus preserving the total magnetization. The sub-Hilbert space consists of the complete set of basis vectors $\{|q_j\rangle\}_{1 \leq j \leq K}$ equipped with $\langle q_i | q_j \rangle = \delta_{i,j}$.

Similarly, if from the fully symmetric state one inverts two spins respectively located at positions j_1 and j_2 the resulting state reads

$$|q_{j_1} + q_{j_2}\rangle = |000 \cdots 1_{j_1} \cdots 1_{j_2} \cdots 000\rangle, \quad (2.22)$$

with $1 \leq j_1 < j_2 \leq K$. The sub-Hilbert space in this sector contains $\binom{K}{2} = K(K-1)/2$ basis vectors i.e. $\{|q_{j_1} + q_{j_2}\rangle\}_{1 \leq j_1 < j_2 \leq K}$ delivered with inner product $\langle q_{j_1} + q_{j_2} | q_{j_1} + q_{j_2} \rangle = \delta_{j_1,j_1} \delta_{j_2,j_2}$. They exactly match the set obtained by addition of two distinct elements in the previous subset. This process can be repeated until the entire set of sub-Hilbert spaces is generated the last but one of which contains $\binom{K}{K-1} = K$ states with $K-1$ spins in up-state

$$|q_{j_1} + q_{j_2} + \cdots + q_{j_{K-1}}\rangle = |1_{j_1} 1_{j_2} \cdots 0 \cdots 1_{j_{K-1}}\rangle, \quad (2.23)$$

with $1 \leq j_1 < j_2 < \cdots < j_{K-1} \leq K$. It should be noted that $|q_{j_1} + q_{j_2} + \cdots + q_{j_K}\rangle = |1_{j_1} 1_{j_2} \cdots 1_{j_K}\rangle \equiv |2^K - 1\rangle$. These observations are useful when it comes to building the eigenvalues and eigenstates of a spin Hamiltonian as shown in next Sections.

In the same logic, excepted for $s_{q_{j_1} + q_{j_2} + \cdots + q_{j_K}}^{(i)+} = 1$, it can easily be seen that

$$s_{q_j}^{(i)+} = \delta_{i,j}, \quad (2.24a)$$

$$s_{q_{j_1} + q_{j_2}}^{(i)+} = \delta_{i,j_1} + \delta_{i,j_2}, \quad (2.24b)$$

$$s_{q_{j_1} + q_{j_2} + q_{j_3}}^{(i)+} = \delta_{i,j_1} + \delta_{i,j_2} + \delta_{i,j_3}, \quad (2.24c)$$

⋮

$$s_{q_{j_1} + q_{j_2} + \cdots + q_{j_{K-1}}}^{(i)+} = \delta_{i,j_1} + \delta_{i,j_2} + \cdots + \delta_{i,j_{K-1}}. \quad (2.24d)$$

Hereby, we verified for further purposes that $\sum_{i=1}^K s_{q_j}^{(i)+} = 1$, $\sum_{i=1}^K s_{q_{j_1} + q_{j_2}}^{(i)+} = 2$ gradually until $\sum_{i=1}^K s_{q_{j_1} + q_{j_2} + \cdots + q_{j_{K-1}}}^{(i)+} =$

$K = 1$. Likewise, considering (B6) one proves that

$$s_{q_j}^{(i)z} = \frac{1}{2} \bar{\delta}_{i,j}, \quad (2.25a)$$

$$s_{q_{j_1}+q_{j_2}}^{(i)z} = \frac{1}{2} (\bar{\delta}_{i,j_1} + \bar{\delta}_{i,j_2}), \quad (2.25b)$$

$$s_{q_{j_1}+q_{j_2}+q_{j_3}}^{(i)z} = \frac{1}{2} (\bar{\delta}_{i,j_1} + \bar{\delta}_{i,j_2} + \bar{\delta}_{i,j_3}), \quad (2.25c)$$

⋮

$$s_{q_{j_1}+q_{j_2}+\dots+q_{j_{K-1}}}^{(i)z} = \frac{1}{2} (\bar{\delta}_{i,j_1} + \bar{\delta}_{i,j_2} + \dots + \bar{\delta}_{i,j_{K-1}}) \quad (2.25d)$$

where we have defined

$$\bar{\delta}_{i,j} = \begin{cases} -1, & i = j \\ +1, & i \neq j \end{cases}, \quad (2.26)$$

Importantly,

$$\bar{\delta}_{i,j} \bar{\delta}_{i,j+1} = \begin{cases} -1, & i = j \\ +1, & i \neq j \end{cases}, \quad (2.27)$$

in opposition to $\delta_{i,j} \delta_{i,j+1} = 0$ as proven below. Thus, because of the constraint $j_1 < j_2$ we always have $\delta_{j_1,j_2} = \delta_{j_1,j_2+1} = 0$ i.e. in general $\delta_{j_k,j_\ell} = \delta_{j_k,j_\ell+1} = 0$ for $k < \ell$; the only contribution coming from $k > \ell$. It is also important for further development to keep in mind that $(1 + \delta_{i,j})(1 - \delta_{i,j}) = (1 - \delta_{i,j})$ and $(1 - \delta_{i,j})(1 - \delta_{i,j}) = (1 - \delta_{i,j})$.

III. APPLICATIONS: 1D SPIN-1/2 INTEGRABLE XXZ HEISENBERG MODEL

In order to illustrate the usefulness of Dirac representation for LSOs we consider the 1D spin-1/2 XXZ Heisenberg model with open boundaries in a magnetic field (MF) and compute its eigenspectrum. Two distinct cases are of interest: the case of uniform and random MFs. For uniform MF (integrable model) the eigenspectrum is in general obtained analytically by invoking the Bethe Anzath[39, 40] which amounts to complicated calculations or by resorting to fermionic or bosonic transformations. We demonstrate that our representation transforms the corresponding eigenvalues problem into recurrence equations that can *easily* be solved. In the case of random MF (non-integrable model) a comprehensive perturbation theory is constructed. The prototype Hamiltonian reads[25, 41]

$$\hat{H} = \sum_{\alpha=x,y,z} \sum_{j=1}^{K-1} J_\alpha \hat{S}_j^\alpha \hat{S}_{j+1}^\alpha + \sum_{j=1}^K h_j \hat{S}_j^z, \quad (3.1)$$

to which we further impose the constraint $J_x = J_y = J$ (anisotropic XXZ spin-1/2) with J measuring spin-spin interactions; J_z is the spin anisotropy parameter, h_j are local magnetic fields applied along the z -direction onto individual spins. Our goal is to revisit this model both

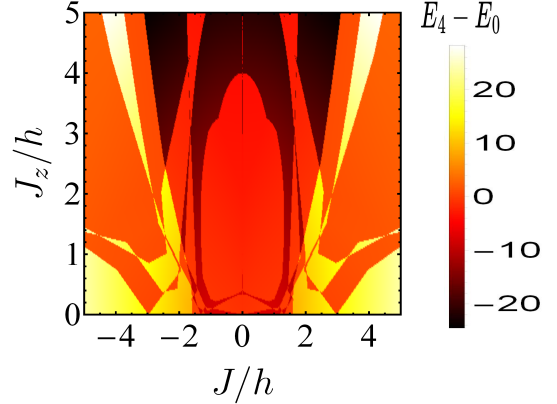


Figure 2. Numerical calculation of the gap $E_4 - E_0$ as a function of the spin-spin exchange J/h and the anisotropy parameter J_z/h in the spin-1/2 XXZ Heisenberg model for $K = 8$ spins. These two parameters conspire in a non-trivial manner leading to the color palette running from -20 to 20 . Three main colors dominate the portrait. From the bottom to the top we go from the minimum to the maximum gap through the red area corresponding to the region where the gap closes ($E_4 - E_0 = 0$). The yellow region corresponds to the region where the gap tends to be maximal while the black region corresponds to the minimum. The presence of fringes is an indication of intrinsic interference pattern i.e. level crossings between E_4 and E_0 by linear variation of J/h . This portrait is not unique, any combination of E_n and E_0 gives a different pattern.

numerically in the Dirac (binary) representation with the aid of exact diagonalization and analytically without invoking neither the Bethe Anzath nor any fermionic or bosonic transformation.

A. Numerical Treatment

Exact diagonalization (ED) in the model (3.1) is achieved by exploiting two main symmetries: the global $U(1)$ and spin-inversion symmetries. These allow us to considerably reduce the size of the Hilbert space. Our choice of spin-spin interaction ensures that \hat{H} has a global $U(1)$ symmetry thus preserving the total magnetization,

$$\hat{\mathcal{J}}^z = \sum_{n=0}^{D-1} m_n^z |n\rangle\langle n|, \quad [\hat{H}, \hat{\mathcal{J}}^z] = 0. \quad (3.2)$$

Here, $m_n^z = \sum_{j=1}^K s_n^{(j)z}$ is the n th magnetic quantum number and written in explicit form in (B22). The conservation (3.2) leads to the Hilbert space fragmentation into disconnected sectors[42, 43]. There are various ways for distinguishing between the sectors. One way consists of labeling them using the total magnetization $\hat{\mathcal{J}}^z$ in which case $-K/2 \leq \hat{\mathcal{J}}^z \leq K/2$ for even number of spins. An alternative way consists of using the number of spins in

either the state $|\uparrow\rangle$ or $|\downarrow\rangle$. We label the sectors with the number K_\uparrow of spins in up-state starting from the smallest values; $0 \leq K_\uparrow \leq K$. The tensor product of subspaces in (2.1) decomposes into direct sum of subspaces as

$$\mathcal{H} = \bigoplus_{j=0}^{K_\uparrow} \mathcal{H}^{(j)}. \quad (3.3)$$

Each subspace is of dimension $\binom{K}{K_\uparrow}$. This is smaller than the 2^K dimension of the original Hilbert space. The Hamiltonian decomposes in a similar fashion. Thanks to this symmetry states with different value of \mathcal{J}^z are not mixed and the Hamiltonian can be diagonalized independently in each subspace. The gaps between the energy of the fourth excited state and the ground-state energies ($E_4 - E_0$) is calculated as a function of J/h and J_z/h and the results are depicted in Fig.2. A similar task is accomplished for $E_8 - E_0$ and displayed in Fig.5. We observe interesting interference patterns revealing the existence of level-crossings between E_4 and E_0 by linear variation of J/h and where the wave functions split and recombine. These calculations can unfortunately only be done for a few number of spins as although exploiting the $U(1)$ global symmetry, ED continues suffering from finite-size effects. We invoke an additional symmetry.

In the absence of local magnetic field, since the system is in addition in an open boundary configuration, it is symmetric under spin-inversion symmetry[29]. The Hamiltonian commutes the spin-inversion operator,

$$\hat{Z} = \sum_{n=0}^{D-1} |D-1-n\rangle\langle n|, \quad [\hat{H}, \hat{Z}] = 0. \quad (3.4)$$

Essentially, $\hat{Z}^\dagger \hat{S}_j^\pm \hat{Z} = \hat{S}_j^\mp$ and $\hat{Z}^\dagger \hat{S}_j^z \hat{Z} = -\hat{S}_j^z$ given in addition that $\hat{Z} = \hat{Z}^{-1} = \hat{Z}^\dagger$ (unitary operator). The operator \hat{Z} is an anti-diagonal matrix that has zeros everywhere excepted on the anti-diagonal where it possesses ones. Therefore, given that $\hat{Z}^2 = I$, its eigenvalues are $z = \pm 1$ and its normalized eigenvectors are

$$|n_z\rangle = \frac{1}{\sqrt{2}}(|n\rangle + z|D-1-n\rangle). \quad (3.5)$$

They are mutually orthogonal and are equipped with a completeness relation that allows them to form a complete set of vectors,

$$\langle m_{z'}|n_z\rangle = \delta_{n,m}\delta_{z,z'}, \quad \sum_{z=\pm 1} \sum_{n=0}^{D-1} |n_z\rangle\langle n_z| = I. \quad (3.6)$$

If one has already implemented the global $U(1)$ symmetry, the spin-inversion symmetry is applicable only in the sector $\mathcal{J}^z = 0$ (largest sector) where

$Z|s_n^{(1)z}, s_n^{(2)z}, \dots, s_n^{(K)z}\rangle = |s_n^{(1)z}, -s_n^{(2)z}, \dots, -s_n^{(K)z}\rangle$. This permits further fragmentation of this subspace into yet two disconnected sectors associated with the eigenvalues z ,

$$\mathcal{H}^{(\mathcal{J}^z=0)} = \mathcal{H}_+ \bigoplus \mathcal{H}_-. \quad (3.7)$$

The projection out of an operator (not necessary a matrix) onto each subspaces can be accomplished with the aid of the projection operator (see also Ref.[44])

$$\hat{\mathcal{P}}_z = \frac{1}{2}(I + z\hat{Z}). \quad (3.8)$$

It is Hermitian with properties $\hat{\mathcal{P}}_z \hat{\mathcal{P}}_{z'} = \delta_{z,z'}$, $\sum_{z=\pm 1} \hat{\mathcal{P}}_z = I$ and $\hat{\mathcal{P}}_z Z = z\hat{\mathcal{P}}_z$. The projection of a (basis) vector initially in the eigenbasis of \mathcal{J}^z onto each new subspace in (3.7) can be realized as

$$|n\rangle = \sum_{z=\pm 1} \sum_{k=0}^{D-1} C_{k_z,n} |k_z\rangle. \quad (3.9)$$

Here, the $C_{k_z,n}$ denoting the projection of $|n\rangle$ onto the direction of $|k_z\rangle$ in the subspace \mathcal{H}_z are determined with the aid of the relations in (3.6) as

$$C_{k_z,n} = \frac{1}{\sqrt{2}}(\delta_{k,n} + z\delta_{k,D-1-n}). \quad (3.10)$$

We see that the basis vectors mix the two subspaces as indicated by $|n\rangle = \frac{1}{\sqrt{2}} \sum_{z=\pm 1} (|n_z\rangle + z|(D-1-n)_z\rangle)$. Every matrix operator $\hat{O} = \sum_{n,m=0}^{D-1} \hat{O}_{n,m} |n\rangle\langle m|$ in the eigenspace (3.3) is projected out onto the eigenspaces \mathcal{H}_z as

$$\hat{O} = \sum_{z',z} \sum_{n,m=0}^{D-1} (\langle \alpha_{z'} | \hat{O} | \beta_z \rangle) |n_z\rangle\langle m_{z'}|, \quad (3.11)$$

where

$$\langle \alpha_{z'} | \hat{O} | \beta_z \rangle = \frac{1}{2} \left(\hat{O}_{\beta,\alpha} + z' \hat{O}_{\beta,D-1-\alpha} + z \hat{O}_{D-1-\beta,\alpha} + zz' \hat{O}_{D-1-\beta,D-1-\alpha} \right), \quad (3.12)$$

are its matrix elements. The $\hat{O}_{\beta,\alpha}$ in the left hand side of (3.12) are components of \hat{O} in the eigenbasis (3.3). In general, \hat{O} mixes states with different z . When it preserves \hat{Z} it does not mix them anymore also falling apart into two disconnected blocks corresponding each to a value of z .

These symmetries have proven in this work to be very powerful in circumventing finite-size effects. Indeed, on a small computer with 32Gb of RAM we have been able on Mathematica 7 to numerically diagonalize \hat{H} for relatively large systems ($K \leq 18$ spins) without resorting to any parallelization. Thanks to the binary representation it only takes a few seconds to build the Hamiltonian as no matrix multiplication is required. We expect to go beyond this value on the C program. The mathematica program is available in the following [GitHub repository](#). Figures 3 and 4 depict our numerical results.

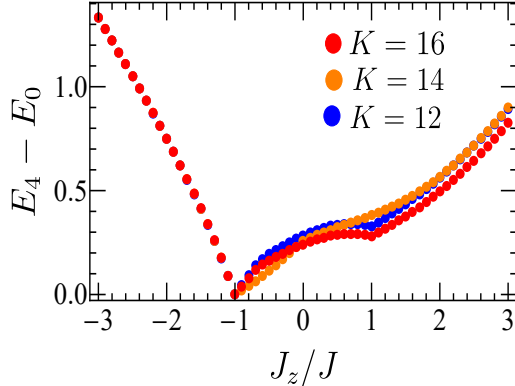


Figure 3. Energy difference $E_4 - E_0$ of the XXZ Heisenberg model with open boundary versus the anisotropy parameter J_z/J for $h = 0.1J$ and various values of the total number of spins. This figure depicts three phases: (i) the regime $J_z/J < -1$ (ferromagnetic gapped phase) where we observe that the gap does not depend on the system size; this is a *bulk gap* as it does not vanish in the thermodynamic limit $K \rightarrow \infty$. We also note that as the anisotropy parameter increases the gap closes and vanishes near $J_z/J = -1$ (critical point) indicating a phase transition. (ii) The regime $-1 < J_z/J \leq 1$ (Luttinger liquid) and (iii) the regime $J_z/J > 1$ (anti-ferromagnetic gapped phase).

B. Analytical Treatment

Now that we have gained insight into the numerical behavior of the generic model \hat{H} , we now aim to obtain its eigenspectrum analytically. In the representation (2.12a)-(2.12c) it casts the form $\hat{H} = \sum_{n=0}^{D-1} \hat{\mathcal{H}}_n$ where

$$\begin{aligned} \hat{\mathcal{H}}_n &= \sum_{j=1}^{K-1} \left(\Delta_n^{(j)+-} |n-Q_j\rangle\langle n| + \Delta_n^{(j)-+} |n+Q_j\rangle\langle n| \right) + \Delta_n^{zz} |n\rangle\langle n|, \\ &= \sum_{j=1}^{K-1} \Delta_n^{(j)-+} (|n\rangle\langle n+Q_j| + |n+Q_j\rangle\langle n|) + \Delta_n^{zz} |n\rangle\langle n|, \end{aligned} \quad (3.13)$$

and where we have defined

$$\Delta_n^{(j)+-} = \frac{J}{2} s_n^{(j)+} s_n^{(j+1)-}, \quad \Delta_n^{(j)-+} = \frac{J}{2} s_n^{(j)-} s_n^{(j+1)+}, \quad (3.14)$$

and the classical Hamiltonian

$$\Delta_n^{zz} = J_z \sum_{j=1}^{K-1} s_n^{(j)z} s_n^{(j+1)z} + \sum_{j=1}^K h_j s_n^{(j)z}, \quad (3.15)$$

with $Q_j = q_j - q_{j+1}$. The quantities $\Delta_n^{(j)+-}$ and $\Delta_n^{(j)-+}$ encapsulate the microscopical structure of neighboring spins in the configuration $|n\rangle$. For parallel neighboring spins $\Delta_n^{(j)+-} = \Delta_n^{(j)-+} = 0$ and $\Delta_n^{(j)+-} = \Delta_n^{(j)-+} = J/2$ for anti-parallel spins. Thus, when neighboring spins are simultaneously inverted, this action interchanges the

quantities in (3.14), $\Delta_{n+Q_j}^{(j)+-} = \Delta_n^{(j)-+}$ and $\Delta_{n-Q_j}^{(j)-+} = \Delta_n^{(j)+-}$. Also, $\Delta_0^{(j)+-} = \Delta_{D-1}^{(j)+-} = 0$ and $\Delta_0^{(j)-+} = \Delta_{D-1}^{(j)-+} = 0$ as all adjacent spins in the states $|0\rangle$ and $|D-1\rangle$ with extremal values of the total magnetization are parallel. We also observe that $\Delta_n^{(j)+-} \cdot \Delta_n^{(j)-+} = 0$ for arbitrary configuration $|n\rangle$ and that $\Delta_n^{(j)+-} = \Delta_{\bar{n}}^{(j)+-}$ and $\Delta_n^{(j)-+} = \Delta_{\bar{n}}^{(j)-+}$ for all lattice site. $(\Delta_n^{(j)+-})^2 = \frac{J}{2} \Delta_n^{(j)+-}$, $(\Delta_n^{(j)-+})^2 = \frac{J}{2} \Delta_n^{(j)-+}$ by virtue of Eq.(B1). Thereby, we infer that $(\Delta_n^{(j)+-})^n = \left(\frac{J}{2}\right)^{n-1} \Delta_n^{(j)+-}$ and $(\Delta_n^{(j)-+})^n = \left(\frac{J}{2}\right)^{n-1} \Delta_n^{(j)-+}$.

Δ_n^{zz} in Eq.(3.15) is nothing but the classical Ising model[45, 46]. It corresponds to the non-interacting limit $J = 0$ of (3.13). When local magnetic fields are randomly distributed as in the MBL case[25, 26], it is equivalent to the Anderson model[47, 48] (single-body localization). Therefore, in this limit a wide class of problems ranging from magnetism[49], phase transitions[50], spin glasses[51] through critical phenomena[52] can easier be handled as there is no need anymore to manipulate quantum but classical objects. We have considerably reduced the level of complexity associated with the quantum nature of spin Hamiltonians. This is clearly an advantage of (3.15) over (3.1). As yet another advantage, we will see later in the work that $\Delta_n^{(j)+-}$ and $\Delta_n^{(j)-+}$ acquire simple forms when we exploit the global $U(1)$ symmetry of \hat{H} by sitting in a given sector of the fragmented Hilbert space. It should be noted for further purposes that $\Delta_0^{zz} = J_z K/4 + \mathbf{h}/2$ and $\Delta_{D-1}^{zz} = -J_z K/4 - \mathbf{h}/2$ with the sample sum $\mathbf{h} = \sum_{j=1}^K h_j$.

A special case of paramount interest to be discussed before diving into the fragmented Hilbert space is the case of *perfect* Neel's states. They correspond to configuration where any adjacent pair of spins are in opposite direction $|\uparrow\downarrow\uparrow\cdots\rangle$ and $|\downarrow\uparrow\downarrow\cdots\rangle$ accounting for the state of the first spin. In other words, $s_{\text{Neel}}^{(j)z} = -s_{\text{Neel}}^{(j+1)z}$. As a consequence, the total magnetization $\mathcal{J}^z = 0$; for every pair $s_{\text{Neel}}^{(j)z} s_{\text{Neel}}^{(j+1)z} = -1/4$, $\Delta_{\text{Neel}}^{(j)+-} = \Delta_{\text{Neel}}^{(j)-+} = J/2$ independently on whether the first component of the chain is found in the state $|\uparrow\rangle$ or $|\downarrow\rangle$ and for homogeneous local magnetic fields $\Delta_{\text{Neel}}^{zz} = -J_z(K-1)/4$. This is an indication that effects of \mathbf{h} in the sector accommodating $|\text{Neel}\rangle$ are suppressed by mutual compensation of flipped spins i.e. $h \sum_{j=1}^{K-1} s_{\text{Neel}}^{(j)z} = h \hat{\mathcal{J}}^z = 0$ for all $|n\rangle$. These remarks confirm that Neel's states (two-fold degenerate) are ground states of the 1D antiferromagnetic spin-1/2 Heisenberg model in the classical limit with energy $\Delta_{\text{Neel}}^{zz}$ [53]. For an even number of spins, $|\text{Neel}\rangle = |\uparrow\downarrow\uparrow\cdots\rangle = |\frac{1}{3}(2^K - 1)\rangle$ and $|\text{Neel}\rangle = |\downarrow\uparrow\downarrow\cdots\rangle = |\frac{1}{3}(2^K - 1)\rangle$.

The central pole of interest in this Section, is the eigenvalue equation $\hat{H}|\psi\rangle = E|\psi\rangle$ with eigenvalue E and the associated eigenstates $|\psi\rangle$. Our goal is to solve this equation. To this end, we recall that in the absence of spin-spin exchange ($J = 0$) spins are in the quantization direction; the eigenvalues of the Hamiltonian are

$E_n = \Delta_n^{zz}$ whilst the eigenstates are $|n\rangle$. When interactions are turned on ($J \neq 0$) spins are in various superpositions of $|n\rangle$ weighted by certain probability amplitudes. The eigenstates of the Hamiltonian can be constructed as,

$$|\psi\rangle = \sum_{n=0}^{D-1} C_n |n\rangle, \quad (3.16)$$

where C_n are projections of $|\psi\rangle$ onto the direction of $|n\rangle$ in the Hilbert space or the probability amplitude of observing spins in the configuration $|n\rangle$. They are subjected to the constraint $\sum_{n=0}^{D-1} |C_n|^2 = 1$. Plugging this into the eigenvalue equation results into the system of recurrence equations

$$\sum_{j=1}^{K-1} \left(\Delta_n^{(j)+-} C_{n+Q_j} + \Delta_n^{(j)-+} C_{n-Q_j} \right) = (E - \Delta_n^{zz}) C_n. \quad (3.17)$$

This equation is reminiscent of the tight-binding problem on a graph. Therefore, the complicated problem of a collection of identical spins interacting pairwise on a simple lattice is transformed into a simple problem of a free spinless particle hopping on a complicated graph as also discussed in Ref.[54].

We solve (3.17) analytically by sitting in each sector of the fragmented Hilbert space. We focus exclusively on even K as the case of odd K follows the same logic. We discriminate between the single-state sectors $K_\uparrow = 0$ and $K_\uparrow = K$ where (3.17) is easily solved as follows:

Sector $K_\uparrow = 0$: This sector has $\binom{K}{0} = 1$ basis vector with fully aligned spins in the state $|\downarrow\rangle$; the so called *pseudo-vacuum state*. Therefore, $|n\rangle \equiv |0\rangle$ and $\Delta_0^{(j)+-} = \Delta_0^{(j)-+} = 0$. The single eigenstate and eigenvalue of the Hamiltonian are respectively $|\psi_0^{(0)}\rangle = |0\rangle$ and $E_0^{(0)} = \Delta_0^{zz} = J_z(K-1)/4 + hK/2$. This emerges as a consequence of the fact that $s_0^{(j)z} = 1/2$ for all j . The superscript on the eigenvalue and the eigenfunction refers to K_\uparrow .

Sector $K_\uparrow = K$: Because this sector has only one state with all spins in the state $|\uparrow\rangle$, same applies. The unique eigenstate and the eigenenergy are respectively $|\psi_{D-1}^{(K)}\rangle = |D-1\rangle$ and $E_{D-1}^{(K)} = \Delta_{D-1}^{zz} = -J_z(K-1)/4 - hK/2$ given that $s_{D-1}^{(j)z} = -1/2$. This is the ground state.

In the remaining sectors, we set $J_z = 0$ for the sake of clarity and simplicity. Interference patterns describing the gap $E_8 - E_0$ for $J_z = 0.7$ is displayed in Fig.5 .

Sector $K_\uparrow = 1$: all $\binom{K}{1} = K$ basis vectors in this sector of the fragmented Hilbert space have one spin in up-state. They can all be built from $|0\rangle$ as $\{|q_i\rangle\}_{1 \leq i \leq K}$ (see previous Section) by flipping one spin. Considering the fact that $\Delta_{q_i}^{(j)+-} \cdot \Delta_{q_i}^{(j)-+} = 0$ as explained earlier, we infer

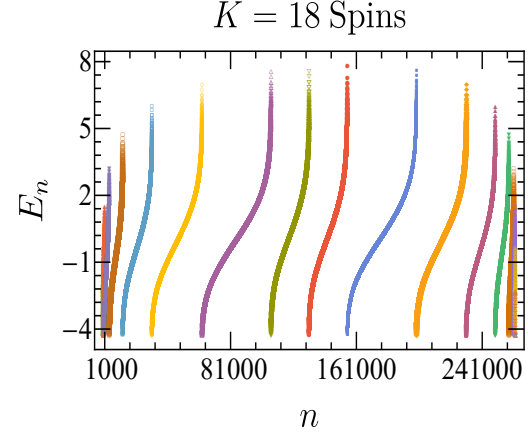


Figure 4. Exact diagonalization results of a spin-1/2 XXZ Heisenberg model of length $K = 18$ for $J_z = -J$ in the absence of local magnetic field $h = 0.0J$. Calculations are numerically done by block-diagonalization of the Hamiltonian and implementation of the spin-inversion symmetry in the sector $\mathcal{J}^z = 0$ i.e. each sector is exactly diagonalized independently. Each colored-solid object corresponds to an eigenvalue of the total magnetization (block).

that $\delta_{i,j}\delta_{i,j+1} = 0$, whereby, it can easily be proven that

$$\Delta_{q_i}^{(j)+-} = \frac{J}{2}\delta_{i,j}, \quad \Delta_{q_i}^{(j)-+} = \frac{J}{2}\delta_{i,j+1}, \quad (3.18)$$

and

$$\Delta_{q_i}^{zz} = h\left(\frac{K}{2} - 1\right), \quad (3.19)$$

Considering now Eqs.(3.18) and (3.19) and because $\Delta_{q_i}^{zz}$ is independent on i it enters Eq.(3.17) as a simple number having only a shift effect. The eigenvalue equation acquires the tight-binding-like form

$$\frac{J}{2} (C_{q_{j-1}} + C_{q_{j+1}}) = EC_{q_j}, \quad (3.20)$$

where here and hereafter one should keep in mind the substitution $E \rightarrow E - \Delta_{q_i}^{zz}$. This is a system of K coupled equations. By virtue of the convention (3.9) they are subject to the constraint $C_{q_0} = C_{q_{K+1}} = 0$. Here, C_{q_j} is the probability amplitude for finding the j th spin in the state up. Its governing equation describes an itinerant particle hopping between neighboring sites $j-1$ and $j+1$ with a hopping integral $J/2$.

Eq.(3.20) can be reduced to a linear three-term recurrence equation by defining $P_j = C_{q_j}$ as $P_{j-1} + P_{j+1} = xP_j$ with $x = 2E/J$. Boundary conditions become $P_0 = P_{K+1} = 0$. This is a state representation as each state $|q_j\rangle$ is now treated as a point j . Upon solving this equation the

eigenfunctions read,

$$|\psi_n^{(1)}\rangle = \frac{1}{N_n} \sum_{j=1}^K P_j(\tilde{E}_n^{(1)})|q_j\rangle, \quad (3.21a)$$

$$N_n = \sqrt{\sum_{j=1}^K |P_j(\tilde{E}_n^{(1)})|^2}, \quad (3.21b)$$

where $\tilde{E}_n^{(1)} = 2E_n^{(1)}/J$ is a dimensionless energy. The Hamiltonian becomes diagonal in the eigenbasis of the corresponding subspace i.e. $H^{(1)} = \sum_{n=0}^{D-1} E_n^{(1)} |\psi_n^{(1)}\rangle\langle\psi_n^{(1)}|$. The superscript refers as usual to the number of spin in up-state.

At this point, it is important to recall that the case $x_j \neq x$ (corresponding to $J_z \neq 0$), although simple at first glance remains till date analytically unsolvable. This could be strange to read but it is the consequence of the fact that the recurrence equation $P_{j-1} + P_{j+1} = x_j P_j$ has no universal solution for arbitrary x_j . In this piece of work, this case is addressed perturbatively with remarkable agreement with the data from exact diagonalization.

For further purposes, it would be interesting to briefly review how the three-term equation for P_j is solved in the homogeneous case. Because this equation is subject to open boundary conditions, a general solution can be constructed as $P_j = \beta^j$ (see Ref.55). Plugging this back into the equation for P_j yields the quadratic equation $\beta^2 - x\beta + 1 = 0$ thence the general solution $P_j = \phi_1(\beta_1)^j + \phi_2(\beta_2)^j$ with $\beta_{1,2} = (x \pm \sqrt{x^2 - 4})/2$. The boundary conditions teach us that $\phi_1 = -\phi_2$ and $(\beta_1/\beta_2)^{K+1} = 1$. We observe that β_1 and β_2 are the roots of unity. They must be complex which can only be realized if $x^2 - 4 < 0$. If we choose $x = 2 \cos \theta$ with $0 \leq \theta \leq \pi$ then $\beta_1 = e^{i\theta}$ and $\beta_2 = e^{-i\theta}$. Hence, $(\beta_1/\beta_2)^{K+1} = e^{2i\pi m}$ with $m = 1, \dots, K$ and whereby $\beta_1/\beta_2 = e^{2i\theta_m}$ with $\theta_m = \pi m/(K+1)$. Thus, $\beta_1^{(m)} = e^{i\theta_m}$, $\beta_2^{(m)} = e^{-i\theta_m}$ and $P_j^{(m)} = A \sin(j\theta_m)$ where A is a normalization constant evaluated from the condition (3.21a). This process yields the eigenvalues[56, 57]

$$E_{q_m}^{(1)} = \Delta_{q_m}^{zz} + J \cos\left(\frac{\pi m}{K+1}\right), \quad (3.22)$$

and the one-particle eigenstates

$$|\psi_{q_m}^{(1)}\rangle = \sum_{j=1}^K u_{j,m}|q_j\rangle, \quad (3.23)$$

where

$$u_{j,m} = \sqrt{\frac{2}{K+1}} \sin\left(\frac{\pi j}{K+1} m\right), \quad (3.24)$$

with $1 \leq m \leq K$. Note that $u_{j,m} = u_{m,j}$ form a structured orthogonal symmetric matrix as explained in Ref.[57].

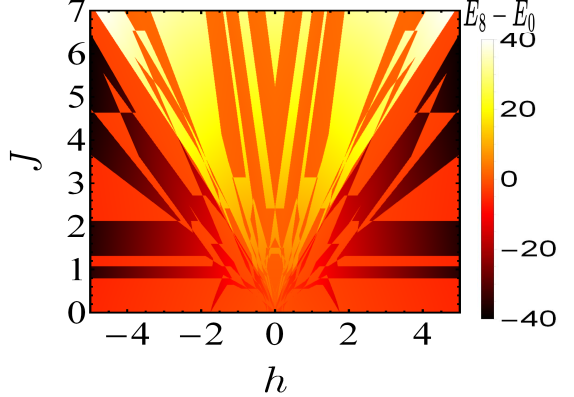


Figure 5. Interference pattern in the gap $E_8 - E_0$ in the XXZ Heisenberg model for $J_z = 0.7$ and $K = 8$. The structure of these patterns suggests the existence of level-crossings ($J < 1$) and avoided-level crossing ($J > 1$) between E_8 and E_0 by variation of h .

The eigenvalues tell us that only the unique spin in up-state in the configuration $|q_j\rangle_{1 \leq j \leq K}$ contributes to the energy. The wave function depends only on the total number of spins.

Sector $K_\uparrow = 2$: In the third sector, all $\binom{K}{2} = K(K-1)/2$ basis vectors have two spins in up-state (two-particle block). The complete set of orthogonal basis vectors in this sector can be obtained from $\{|q_{j_1} + q_{j_2}\rangle\}_{1 \leq j_1 < j_2 \leq K}$ corresponding to all distinct ways of arranging two spins in up-state in a chain of $K-2$ spins in down-state. Hence,

$$\Delta_{q_{j_1} + q_{j_2}}^{(j)+-} = \frac{J}{2} [\delta_{j_1,j}(1 - \delta_{j_2,j+1}) + \delta_{j_2,j}(1 - \delta_{j_1,j+1})], \quad (3.25a)$$

$$\Delta_{q_{j_1} + q_{j_2}}^{(j)-+} = \frac{J}{2} [\delta_{j_1,j+1}(1 - \delta_{j_2,j}) + \delta_{j_2,j+1}(1 - \delta_{j_1,j})], \quad (3.25b)$$

and

$$\Delta_{q_{j_1} + q_{j_2}}^{zz} = h \left(\frac{K}{2} - 2 \right). \quad (3.26)$$

It should be noted that under the constraint $i < j$ the term $\delta_{i,j+1}$ contributes only for $i \geq 2$. Indeed, for $i = 1$ there is no value of j such that $i = j+1$. Taking this remark into account Eq.(3.17) then takes the form

$$\begin{aligned} \frac{J}{2} [(1 - \delta_{j_1-1,j_2}) C_{q_{j_1-1} + q_{j_2}} + (1 - \delta_{j_1+1,j_2}) C_{q_{j_1+1} + q_{j_2}}] + \\ \frac{J}{2} [(1 - \delta_{j_1,j_2-1}) C_{q_{j_1} + q_{j_2-1}} + (1 - \delta_{j_1,j_2+1}) C_{q_{j_1} + q_{j_2+1}}] = EC_{q_{j_1} + q_{j_2}}. \end{aligned} \quad (3.27)$$

This equation is solved with the conditions $C_{q_0 + q_{j_2}} = C_{q_{j_1} + q_0} = 0$ and $C_{q_{K+1} + q_{j_2}} = C_{q_{j_1} + q_{K+1}} = 0$ for $j_1 < j_2$. As we did for the second sector, we define the auxiliary variable $P_{j_1,j_2} = C_{q_{j_1} + q_{j_2}}$ and obtain the two-dimensional

linear recurrence equation

$$\begin{aligned} & \left[(1 - \delta_{j_1-1, j_2}) P_{j_1-1, j_2} + (1 - \delta_{j_1+1, j_2}) P_{j_1+1, j_2} \right] + \\ & \left[(1 - \delta_{j_1, j_2-1}) P_{j_1, j_2-1} + (1 - \delta_{j_1, j_2+1}) P_{j_1, j_2+1} \right] = x P_{j_1, j_2}, \end{aligned} \quad (3.28)$$

with boundary conditions $P_{0, j_2} = P_{j_1, 0} = P_{K+1, j_2} = P_{j_1, K+1} = 0$. Once this equation is solved, the eigenvectors are calculated as

$$|\psi_n^{(2)}\rangle = \frac{1}{N_n} \sum_{1 \leq j_1 < j_2 \leq K} P_{j_1, j_2} (\tilde{E}_n) |q_{j_1} + q_{j_2}\rangle, \quad (3.29a)$$

$$N_n = \sqrt{\sum_{1 \leq j_1 < j_2 \leq K} |P_{j_1, j_2} (\tilde{E}_n)|^2}. \quad (3.29b)$$

By virtue of the condition $j_1 < j_2$ it is legitimate to set $P_{j, j} = 0$. Therefore, all Kronecker delta terms in Eq.(3.28) do not contribute. For example $\delta_{j_1-1, j_2} P_{j_1-1, j_2} = \delta_{j_1+1, j_2} P_{j_1+1, j_2} = 0$; this is the consequence of the fact that in such terms every attempt of Kronecker delta to contribute is immediately multiplied by $P_{j, j} = 0$. These observations greatly simplify Eq.(3.28) leading to,

$$[P_{j_1-1, j_2} + P_{j_1+1, j_2}] + [P_{j_1, j_2-1} + P_{j_1, j_2+1}] = x P_{j_1, j_2}. \quad (3.30)$$

Here, it can be observed that the first brackets gather all terms with the same index j_2 while the second one is for those with the same j_1 . It can then be solved by separating the variable as $P_{j_1, j_2} = X_{j_1} Y_{j_2}$. Inserting this into (3.30) and dividing the resulting equation by P_{j_1, j_2} we find that the consistency of the leading equation is achieved when $X_{j_1-1} - \eta X_{j_1} + X_{j_1+1} = 0$ and $Y_{j_2-1} - (x - \eta) Y_{j_2} + Y_{j_2+1} = 0$ with η an arbitrary parameter. These equations are respectively solved with boundary conditions $X_0 = X_{K+1} = 0$ and $Y_0 = Y_{K+1} = 0$. We have then transformed (3.30) into two uncoupled linear recurrence equation each describing the sector $K_\uparrow = 1$. We obtain the eigenvalues

$$E_{m_1, m_2}^{(2)} = \Delta_{q_{m_1} + q_{m_2}}^{zz} + J \cos\left(\frac{\pi m_1}{K+1}\right) + J \cos\left(\frac{\pi m_2}{K+1}\right), \quad (3.31)$$

and eigenstates

$$|\psi_{m_1, m_2}^{(2)}\rangle = \sum_{1 \leq j_1 < j_2 \leq K} u_{j_1, m_1} u_{j_2, m_2} |q_{j_1} + q_{j_2}\rangle. \quad (3.32)$$

However, (3.32) is not the correct expression for eigenstates. Indeed, because local spins are indistinguishable, the wave function should only change by a factor when interchanging particles with spins pointing in the same direction i.e. $|\psi_{m_1, m_2}^{(2)}\rangle = e^{i\phi} \psi_{m_2, m_1}^{(2)}$. For states in the sectors $K_\uparrow = 0$ and $K_\uparrow = K$ (fully symmetric states) the phase ϕ is chosen as $\phi = 0$ while for states in other sectors, the wave function must be anti-symmetric by interchanging particles. The phase is chosen as $\phi = \pi$ and,

$$|\psi_{m_1, m_2}^{(2)}\rangle = -|\psi_{m_2, m_1}^{(2)}\rangle. \quad (3.33)$$

This is referred in quantum mechanics to as Pauli's exclusion principle[58]. For our construction (3.32), we observe that the two-particle wave function does not fulfill the anti-symmetric requirement (3.33). This problem is circumvent by re-constructing the wave function as the linear combination of the two solutions in (3.33) i.e.

$$|\psi_{\mathbf{m}}^{(2)}\rangle = \sum_{1 \leq j_1 < j_2 \leq K} D_{m_1, m_2}^{j_1, j_2} |q_{j_1} + q_{j_2}\rangle, \quad (3.34)$$

where

$$D_{m_1, m_2}^{j_1, j_2} = \begin{vmatrix} u_{j_1, m_1} & u_{j_1, m_2} \\ u_{j_2, m_1} & u_{j_2, m_2} \end{vmatrix} = \sum_{i,j=1}^2 \epsilon_{i,j} u_{j_1, m_i} u_{j_2, m_j}, \quad (3.35)$$

is nothing but the two-particle Slater determinant[58] and $\mathbf{m} = q_{m_1} + q_{m_2}$ with $1 \leq m_1 < m_2 \leq K$. In these expressions $j_2 = j_1 + 1$ such that for a function g_{j_1, j_2} the double summation in (3.34) can be viewed as $\sum_{1 \leq j_1 < j_2 \leq K} g_{j_1, j_2} = \sum_{j_1=1}^K \sum_{j_2=j_1+1}^K g_{j_1, j_2}$. In Eq.(3.35)

$$\epsilon_{i,j} = \begin{cases} +1, & \text{if } (i,j) = (1,2), \\ -1, & \text{if } (i,j) = (2,1), \\ 0, & \text{if } i = j \end{cases} \quad (3.36)$$

is the two-dimensional Levi-Civita symbol. The Slater determinant vanishes by repetition of two indices, $D_{m, m}^{j_1, j_2} = D_{m_1, m_2}^{j_1, j_2} = D_{m, m}^{j_2, j_1} = 0$.

At this stage, one might be tempted to conjecture about the global structure of the eigensystem. However, in order to ensure a better understanding, it is preferable to first gain further insight into the general structure of the recurrence equation by briefly examining the sector with three spins in the up-state.

Sectors $K_\uparrow = 3$: The sub-Hilbert space corresponds to all possible manners of replacing three spins in a spin chain with K identical spins in down-state with three spins in up-state. It can quickly be verified that

$$\Delta_{q_{j_1}+q_{j_2}+q_{j_3}}^{(j)+-} = \frac{J}{2} [\delta_{j_1,j} (1 - \delta_{j_2,j+1} - \delta_{j_3,j+1}) + \delta_{j_2,j} (1 - \delta_{j_1,j+1} - \delta_{j_3,j+1}) + \delta_{j_3,j} (1 - \delta_{j_1,j+1} - \delta_{j_2,j+1})], \quad (3.37a)$$

$$\Delta_{q_{j_1}+q_{j_2}+q_{j_3}}^{(j)-+} = \frac{J}{2} [\delta_{j_1,j+1} (1 - \delta_{j_2,j} - \delta_{j_3,j}) + \delta_{j_2,j+1} (1 - \delta_{j_1,j} - \delta_{j_3,j}) + \delta_{j_3,j+1} (1 - \delta_{j_1,j} - \delta_{j_2,j})]. \quad (3.37b)$$

In the same fashion as we did for previous sectors, this leads to the three-dimensional linear recurrence equation

$$\begin{aligned} & [(1 - \delta_{j_1-1,j_2} - \delta_{j_1-1,j_3}) P_{j_1-1,j_2,j_3} + (1 - \delta_{j_1+1,j_2} - \delta_{j_1+1,j_3}) P_{j_1+1,j_2,j_3}] + \\ & [(1 - \delta_{j_2-1,j_1} - \delta_{j_2-1,j_3}) P_{j_2-1,j_1,j_3} + (1 - \delta_{j_2+1,j_1} - \delta_{j_2+1,j_3}) P_{j_2+1,j_1,j_3}] + \\ & [(1 - \delta_{j_3-1,j_1} - \delta_{j_3-1,j_2}) P_{j_3-1,j_1,j_2} + (1 - \delta_{j_3+1,j_1} - \delta_{j_3+1,j_2}) P_{j_3+1,j_1,j_2}] = x P_{j_1,j_2,j_3}. \end{aligned} \quad (3.38)$$

This equation is solved with boundary conditions $P_{0,j_2,j_3} = P_{j_1,0,j_3} = P_{j_1,j_2,0} = 0$ and $P_{K+1,j_2,j_3} = P_{j_1,K+1,j_3} = P_{j_1,j_2,K+1} = 0$. It is important to go deep into this case in order to have a clear comprehension of our ongoing strategy. As in previous cases and by virtue of the assumption $j_1 < j_2 < j_3$ we can assume that $P_{j_1,j_2,j_3} = 0$ for every repeated (two or more) indices. For example $P_{j_1,j_1,j_3} = P_{j_1,j_1,j_1} = P_{j_1,j_2,j_2} = 0$ and many more. Hence, all Kronecker delta term in (3.38) vanish leading us to

$$\begin{aligned} & [P_{j_1-1,j_2,j_3} + P_{j_1+1,j_2,j_3}] + [P_{j_2-1,j_1,j_3} + P_{j_1+1,j_2,j_3}] \\ & + [P_{j_3-1,j_1,j_2} + P_{j_3+1,j_1,j_2}] = x P_{j_1,j_2,j_3}. \end{aligned} \quad (3.39)$$

By separation of variable as we did so far, one achieves a set of three uncoupled linear-recurrence equations that are solved exactly as for the case of $K_\uparrow = 1$. This task leads to an eigensystem similar to (3.31) and (3.32). Hence, $|\psi_{m_1,m_2,m_3}^{(3)}\rangle = \sum_{1 \leq j_1 < j_2 < j_3 \leq K} u_{j_1,m_1} u_{j_2,m_2} u_{j_3,m_3} |q_{j_1} + q_{j_2} + q_{j_3}\rangle$. As already pinpointed, such a wave function does not fulfill the fundamental principle of indistinguishability of particles. Upon overcoming this constraint through the three-particle Slater determinant[58] we obtain

$$|\psi_{m_1,m_2,m_3}^{(2)}\rangle = \sum_{1 \leq j_1 < j_2 < j_3 \leq K} D_{m_1,m_2,m_3}^{j_1,j_2,j_3} |q_{j_1} + q_{j_2} + q_{j_3}\rangle, \quad (3.40)$$

where

$$\begin{aligned} D_{m_1,m_2,m_3}^{j_1,j_2,j_3} &= \begin{vmatrix} u_{j_1,m_1} & u_{j_1,m_2} & u_{j_1,m_3} \\ u_{j_2,m_1} & u_{j_2,m_2} & u_{j_2,m_3} \\ u_{j_3,m_1} & u_{j_3,m_2} & u_{j_3,m_3} \end{vmatrix} \\ &= \sum_{i,j,k=1}^3 \epsilon_{i,j,k} u_{j_1,m_i} u_{j_2,m_j} u_{j_3,m_k}. \end{aligned} \quad (3.41)$$

Here, $\epsilon_{i,j,k}$ is the three-dimensional Levi-Civita symbol. For a given function g_{j_1,j_2,j_3} the triple summation in (3.40) can be replaced as $\sum_{1 \leq j_1 < j_2 < j_3 \leq K} g_{j_1,j_2,j_3} = \sum_{j_1=1}^K \sum_{j_2=j_1+1}^K \sum_{j_3=j_2+1}^K g_{j_1,j_2,j_3}$.

We are now in position to extend our analysis to arbitrary sector $1 \leq K_\uparrow \leq K - 1$. In order to achieve this goal

and for $1 \leq j_1 < j_2 < \dots < j_{K_\uparrow} \leq K$ we have to write our classical variables in each sector. Thus, in general,

$$\Delta_{q_{j_1}+q_{j_2}+q_{j_3}+\dots+q_{j_{K_\uparrow}}}^{(j)+-} = \frac{J}{2} \sum_{\ell=1}^{K_\uparrow} \delta_{j_\ell,j} \mathcal{X}_{j_\ell+1}, \quad (3.42)$$

$$\Delta_{q_{j_1}+q_{j_2}+q_{j_3}+\dots+q_{j_{K_\uparrow}}}^{(j)-+} = \frac{J}{2} \sum_{\ell=1}^{K_\uparrow} \delta_{j_\ell,j+1} \mathcal{X}_{j_\ell}, \quad (3.43)$$

$$\Delta_{q_{j_1}+q_{j_2}+q_{j_3}+\dots+q_{j_{K_\uparrow}}}^{zz} = h \left(\frac{K}{2} - K_\uparrow \right), \quad (3.44)$$

where we have defined

$$\mathcal{X}_{j_\ell \pm 1} = \left(1 - \sum_{k \neq \ell}^{K_\uparrow} \delta_{j_k,j_\ell \pm 1} \right), \quad (3.45)$$

and where $f_{j_\ell} = (\delta_{j_\ell,1} - \delta_{j_\ell,K})/2$ is associated with spin chain's gates; $j = 1$ ($f_1 = 1/2$) and $j = K$ ($f_K = -1/2$) are respectively the left and right gates. The region $1 < j < K$ is the active domain where $f_j = 0$.

Owing to the important fact that $\delta_{j_k,j} \delta_{j_k,j+1} = 0$ as indicated earlier the eigenvalues equation (3.17) takes the generalized form,

$$\sum_{\ell=1}^{K_\uparrow} \left(\mathcal{X}_{j_\ell-1} P_{j_\ell-1,\dots,j_{K_\uparrow}} + \mathcal{X}_{j_\ell+1} P_{j_\ell+1,\dots,j_{K_\uparrow}} \right) = x P_{j_1,\dots,j_{K_\uparrow}}, \quad (3.46)$$

i.e.

$$\sum_{\ell=1}^{K_\uparrow} \left(P_{j_\ell-1,\dots,j_{K_\uparrow}} + P_{j_\ell+1,\dots,j_{K_\uparrow}} \right) = x P_{j_1,\dots,j_{K_\uparrow}}, \quad (3.47)$$

and is associated with the traditional boundary conditions $P_{0,j_2,\dots,j_{K_\uparrow}} = P_{j_1,0,\dots,j_{K_\uparrow}} = \dots = P_{j_1,j_2,\dots,0} = 0$ and $P_{K+1,j_2,\dots,j_{K_\uparrow}} = P_{j_1,K+1,\dots,j_{K_\uparrow}} = \dots = P_{j_1,j_2,\dots,K+1} = 0$. Eq.(3.47) arises as a consequence of the fact that all Kronecker delta terms vanish following from $1 \leq j_1 < j_2 < \dots <$

$j_K \leq K_\uparrow$ and the introduction of the auxiliary variable $P_{j_1, \dots, j_{K_\uparrow}} = C_{q_{j_1} + q_{j_2} + \dots + q_{j_\ell} + \dots + q_{j_{K_\uparrow}}}$.

Upon solving Eq.(3.47) by variable separation as promoted so far leads us independently on the sector to the eigenenergies,

$$E_n = \Delta_n^{zz} + J \sum_{j=1}^K s_n^{(j)+} \cos\left(\frac{\pi j}{K+1}\right). \quad (3.48)$$

Here, $s_n^{(j)+}$ and $s_n^{(j)z}$ are classical spins in (2.13a) and (2.13c) respectively. This relation is reminiscent of the second equation in (2.7) where now the cos-function plays the role of q_j . By setting $n = \{q_j\}_{1 \leq j \leq K}$ as in the sector $K_\uparrow = 1$ or $n = \{q_{j_1} + q_{j_2}\}_{1 \leq j_1 < j_2 \leq K}$ as in the sector $K_\uparrow = 2$ etc and accounting for (2.24) we retrieve previous results. We observe that the energy linearly changes with J .

Our general results for the eigenstates exclude the sectors with extremal value of the total magnetization as they contain fully-symmetric states. They are written here as

$$|\psi_{\mathbf{n}_i}^{(K_\uparrow)}\rangle = \sum_{\mathbf{j}} D_{\mathbf{i}, \mathbf{j}}^{(K_\uparrow)} |\mathbf{n}_j\rangle, \quad (3.49)$$

where

$$D_{\mathbf{i}, \mathbf{j}}^{(K_\uparrow)} = \sum_{i_1, i_2, \dots, i_{K_\uparrow}=1}^{K_\uparrow} \epsilon_{i_1, i_2, \dots, i_{K_\uparrow}} u_{j_1, m_{i_1}} u_{j_2, m_{i_2}} \dots u_{j_{K_\uparrow}, m_{i_{K_\uparrow}}}, \quad (3.50)$$

is the multi-particle Slater determinant[58] with $D_{\mathbf{i}, \mathbf{j}}^{(K)} = 1$. Here, $\mathbf{i} = \{i_1, i_2, \dots, i_{K_\uparrow}\}$, $\mathbf{j} = \{j_1, j_2, \dots, j_{K_\uparrow}\}$; $\mathbf{n}_k = q_{k_1} + \dots + q_{k_{K_\uparrow}}$ with $\mathbf{k} \in (\mathbf{i}, \mathbf{j})$; $1 \leq i_1 < i_2 < \dots < i_{K_\uparrow} \leq K$ and $1 \leq j_1 < j_2 < \dots < j_{K_\uparrow} \leq K$ (see also Refs.[55, 57]). The multi-dimensional Levi-Civita $\epsilon_{i_1, i_2, \dots, i_{K_\uparrow}} = 0$ if any two indices are the same; $\epsilon_{i_1, i_2, \dots, i_{K_\uparrow}} = +1$ for even permutation of $(1, 2, \dots, K_\uparrow)$; $\epsilon_{i_1, i_2, \dots, i_{K_\uparrow}} = -1$ for odd permutation of $(1, 2, \dots, K_\uparrow)$.

IV. NON-INTEGRABLE VERSION

We have so far discussed the integrable version of (3.1) and got full access to its eigenspectrum in some specific cases. Although this helps gaining insight into the physics of spin systems, physics could radically be different when systems are found in more realistic situations. For example spins systems contaminated with sufficiently strong disorder exhibit Many-Body localization losing their ability to thermalize and explore their entire Hilbert space[25, 26]. This leads to a new phase of matter. Understanding this phenomenon requires analyzing energy-level spacing or inverse participation ratios (IPR)[59, 60]. The method presented

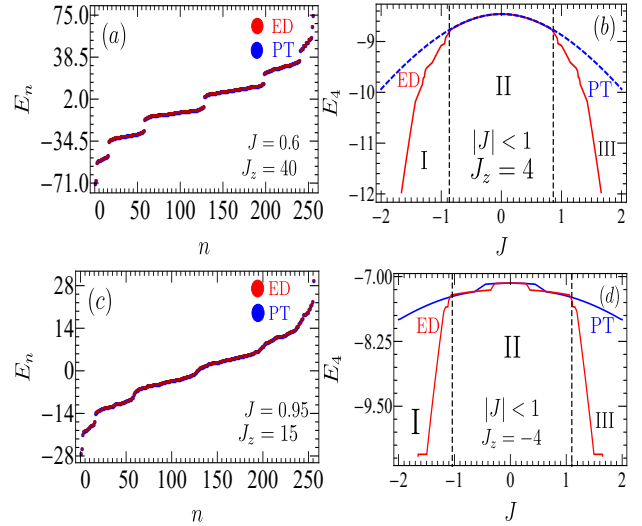


Figure 6. **Left-Panel:** Results of exact diagonalization (ED) versus data from perturbation theory (PT) for the random spin-1/2 XXZ Heisenberg model with open boundary conditions[61]. We observe that both data are barely discernible. The values are sorted in ascendant order and this explains why the branches $E_n < 0$ and $E_n > 0$ have disappeared. **Right-Panel:** Range of validity of our PT. We confirm that our PT is valid in the region II ($|J| < 1$ and arbitrary J_z). It completely fails in the regions I and III. Local magnetic fields (disorder) are withdrawn from a uniform distribution $[-h, h]$. For calculations, we choose $h = 3$ and restricted ourselves to small spin system ($K = 8$) for the sake of clarity of figures.

above fails as a consequence of the fact that the h_j are all distinct and the anisotropy parameter playing a crucial role leads to tight-binding equations that cannot be solved in compact form. It is commonly desired in such cases to use exact-diagonalization (ED) to evaluate the eigenspectrum in order to discriminate between ergodic and MBL phases and predict the critical value of disorder at which transition between the two phases occurs. As already mentioned the exponential growth of the Hilbert space with the total number of spins, causes finite-size effects dramatically limiting the number of implementable spins. The strongest methods amounting for large computer memory and exceeding long time can handle only up to $K = 24$ spins (to the best of our knowledge) provided one can identify and exploit certain symmetries as we did in Section III.

We propose in this Section to perturbatively calculate the eigenspectrum (up to the fourth order) of the spin-1/2 random XXZ Heisenberg model (3.1) in an open boundary configuration. Analytical expressions are written down and could be used to dig deeper into MBL. Our results are confirmed with data from ED in small chains and could easily be extended to arbitrary K by simply setting the desired value of K into our expressions.

A perturbation theory including higher order is elaborated in Appendix C. As traditionally required, the Hamiltonian is split into an unperturbed part \hat{H}_0 whose spectrum is well-identified and a perturbed part \hat{H}_1 with respect to a perturbative parameter. For our case, $\hat{H}_0 = J_z \sum_{j=1}^{K-1} \hat{S}_j^z \hat{S}_{j+1}^z + \sum_{j=1}^K h_j \hat{S}_j^z$ is diagonal with entries Δ_n^{zz} in Eq.(3.15) assumed to be real and non-degenerate, J is the perturbative parameter while $\hat{H}_1 = \sum_{j=1}^{K-1} (\hat{S}_j^x \hat{S}_{j+1}^x + \hat{S}_j^y \hat{S}_{j+1}^y)$ with the structured symmetric matrix elements $X_{n,m} = \langle n | \hat{H}_1 | m \rangle$ given by,

$$X_{n,m} = J^{-1} \sum_{j=1}^{K-1} \left(\Delta_m^{(j)+-} \delta_{n,m-Q_j} + \Delta_m^{(j)-+} \delta_{n,m+Q_j} \right). \quad (4.1)$$

In the Dirac representation, we see that $X_{n,m}$ can be regarded as a generalized hopping model where $\Delta_m^{(j)+-}$ and $\Delta_m^{(j)-+}$ determine the hopping amplitude between neighboring sites separated by Q_j such that $X_{n,n+Q_j} = \Delta_{n+Q_j}^{(j)+-} = \Delta_n^{(j)-+}$ and $X_{n,n-Q_j} = \Delta_{n-Q_j}^{(j)+-} = \Delta_n^{(j)+-}$. Note that $X_{n,n} = 0$ typically because $Q_j > 0$ and there is no j in the interval $1 \leq j \leq K-1$ for which $\delta_{n,n+Q_j} = \delta_{n,n-Q_j} = 1$.

For our perturbative analysis, we are interested in the energy and wave function of the n th configuration determined up to a certain order as

$$E_n \approx \sum_{k=0}^3 J^k \mathcal{E}_n^{(k)} + \mathcal{O}(J^4), \quad (4.2)$$

$$|\psi_n\rangle \approx \sum_{k=0}^2 J^k |\psi_n^{(k)}\rangle + \mathcal{O}(J^3). \quad (4.3)$$

Here, $\mathcal{E}_n^{(k)}$ and $|\psi_n^{(k)}\rangle$ are the k -order corrections to the energy and eigenstates respectively. The superscripts are not to be confused with sectors and in what follows the subscripts m do not refer to the magnetic quantum number. Foremost, we start by describing the energy. According to the perturbation theory in Appendix C the zero-order contribution to the energy corresponds to the eigenvalue of \hat{H}_0 and reads $\mathcal{E}_n^{(0)} = \Delta_n^{zz}$ while the first order $\mathcal{E}_n^{(1)} = X_{n,n} = 0$ for the aforementioned reasons. Other contributions write

$$\mathcal{E}_n^{(2)} = \sum_{n \neq m=0}^{D-1} \frac{X_{n,m} X_{m,n}}{\Lambda_{n,m}}, \quad (4.4)$$

and

$$\mathcal{E}_n^{(3)} = \sum_{m_1 \neq n=0}^{D-1} \sum_{m_2 \neq n=0}^{D-1} \frac{X_{n,m_1} X_{m_1,m_2} X_{m_2,n}}{\Lambda_{n,m_1} \Lambda_{n,m_2}}, \quad (4.5)$$

where $\Lambda_{n,m}$ denotes the energy difference (gap) $\Lambda_{n,m} = \Delta_n^{zz} - \Delta_m^{zz}$ between the configurations $|n\rangle$ and $|m\rangle$. It is also

the energy accumulated by the system when transitioning from $|n\rangle$ and $|m\rangle$ vice versa. Note that when $J = 0$ (Anderson limit) no transition between the eigenstates of \hat{H}_0 occurs, $E_n = \Delta_n^{zz}$ as all corrections vanish, the system remains in its original configuration. Our perturbation treatment completely fails in describing Anderson localization.

In the expression for the eigenstates, the zero-order correction corresponds to the eigenstate of \hat{H}_0 namely $|\psi_n^{(0)}\rangle = |n\rangle$ whereas the first and second order contributions are respectively given by

$$|\psi_n^{(1)}\rangle = \sum_{m \neq n}^{D-1} \frac{X_{n,m}}{\Lambda_{n,m}} |m\rangle, \quad (4.6)$$

and

$$|\psi_n^{(2)}\rangle = \sum_{m \neq n}^{D-1} \sum_{m_1 \neq n}^{D-1} \frac{X_{n,m_1} X_{m_1,m}}{\Lambda_{n,m_1} \Lambda_{n,m}} |m\rangle - \frac{1}{2} \left(\sum_{m \neq n}^{D-1} \frac{X_{n,m} X_{m,n}}{\Lambda_{n,m}^2} \right) |n\rangle. \quad (4.7)$$

Albeit the above expressions can readily be implemented in any symbolic calculator, our preeminent goal is to analytically calculate them and break them down into sectors corresponding to fixed values of the magnetic quantum number.

1. Eigenenergies

We start with the eigenenergies. Thanks to the hopping-shaped form of $X_{n,m}$ in terms of Kronecker Delta symbols plugging this back into Eq.(4.4) allows us after a few calculations to find that:

$$\mathcal{E}_n^{(2)} = \sum_{j=1}^{K-1} \left(\frac{\left(\Delta_n^{(j)-+} \right)^2}{\Lambda_{n,n+Q_j}} + \frac{\left(\Delta_n^{(j)+-} \right)^2}{\Lambda_{n,n-Q_j}} \right). \quad (4.8)$$

Similarly, it is proven with less effort that $\mathcal{E}_n^{(3)} = 0$. As a consequence of these results, the energy holds up to the order $\mathcal{O}(J^4)$. Using the properties $(\Delta_n^{(j)-+})^2 = \frac{J}{2}(\Delta_n^{(j)+-})$ and $(\Delta_n^{(j)+-})^2 = \frac{J}{2}(\Delta_n^{(j)-+})$ as elaborated in the Subsection III B yields,

$$E_n \approx \Delta_n^{zz} + \frac{J}{2} \sum_{j=1}^{K-1} \left(\frac{\Delta_n^{(j)-+}}{\Lambda_{n,n+Q_j}} + \frac{\Delta_n^{(j)+-}}{\Lambda_{n,n-Q_j}} \right) + \mathcal{O}(J^4). \quad (4.9)$$

This result is tested numerically and is valid for $|J| \leq 1$ and arbitrary $|J_z|$ as depicted in Fig.6. We observe that the eigenenergies greatly converge to the exact diagonalization results. This is a consequence of the fact that $\mathcal{E}_n^{(1)} = \mathcal{E}_n^{(3)} = 0$ leading to a high correction. We also observe from Fig.6(a) that for large anisotropy ($J_z \gg 1$) when E_n are sorted in ascendant order as a function n

they depict several clusters where energies are nearly degenerate. This behavior disappears for small and moderate anisotropy as shown in Fig.6(c).

Despite the above observations, it remains of paramount importance to break (4.9) down into sectors. To this end, we first prove that for $1 \leq K_{\uparrow} \leq K - 1$ and $1 \leq j_1 < j_2 < \dots < j_{K_{\uparrow}} \leq K - 1$,

$$\Delta_{q_{j_1}+q_{j_2}+\dots+q_{j_{K_{\uparrow}}}}^{zz} = \left(\frac{\mathbf{h}}{2} - \sum_{k=1}^{K_{\uparrow}} h_{j_k} \right) + J_z \left(\frac{K-1}{4} - K_{\uparrow} \right) + J_z \sum_{\ell=1}^{K_{\uparrow}} \left(f_{j_{\ell}} + \sum_{k \neq \ell}^{K_{\uparrow}} \delta_{j_k, j_{\ell+1}} \right). \quad (4.10)$$

This expression is extended to the last spin i.e. $1 \leq j_1 < j_2 < \dots < j_{K_{\uparrow}} \leq K$ by replacing $f_{j_{\ell}}$ by $g_{j_{\ell}} = (\delta_{j_{\ell}, 1} + \delta_{j_{\ell}, K})/2$.

It should be noted that the second order correction (4.8) has the same structure as (3.17). $\mathcal{E}_n^{(2)}$ is therefore expected in each sector to cast the form of the relations for P_j as shown below.

Sector $K_{\uparrow} = 1$: In this sector, classical variables are given by Eq.(3.18). The energy of the system reads,

$$E_{q_j}^{(K_{\uparrow}=1)} \approx \Delta_{q_j}^{zz} + (W_{j, j-1} + W_{j, j+1}) + \mathcal{O}(J^4), \quad (4.11)$$

where

$$\Delta_{q_j}^{zz} = \left(\frac{\mathbf{h}}{2} - h_j \right) + J_z \left(\frac{K-1}{4} - 1 \right) + J_z g_j, \quad (4.12)$$

and

$$W_{i,j} = -\frac{\left(\frac{J}{2}\right)^2}{(h_i - h_j) - J_z(g_i - g_j)}, \quad (4.13)$$

is defined such that $W_{i,0} = W_{i,K+1} = W_{i,i} = 0$. Eq.(4.11) is reminiscent of a 1D semi-classical tight-binding model for a free traveling particle. In this context, $\Delta_{q_j}^{zz}$ plays the role of the onsite energy while the dimensionless parameter $W_{i,j}$ depicts the interplay between interactions and disorder on one hand, disorder and anisotropy on the other hand and can be interpreted as the transfer rate between the states $|q_i\rangle$ and $|q_j\rangle$. Population transfer is done by successive jumps between neighboring states. These results could be interesting in deciphering the complex mechanism behind MBL in spin chains. For example, for a sample drawn from a uniform distribution, we have calculated in inverse participation ratio (IPR) in Fig.7 for 500 realizations. We see that the wave function tend to concentrate in certain regions than the others indicating the existence of localization.

Sector $K_{\uparrow} = 2$: In this subspace, $\Delta_{q_{j_1}+q_{j_2}}^{(j)+}$ and $\Delta_{q_{j_1}+q_{j_2}}^{(j)-}$ are given by (3.25) while $\Delta_{q_{j_1}+q_{j_2}}^{zz}$ can easily be inferred from (4.10). As a result of substituting the correspond-

ing expressions into (4.9) one obtains

$$\begin{aligned} & \left[(1 - \delta_{j_1-1, j_2}) W_{j_1-1, j_2} + (1 - \delta_{j_1+1, j_2}) W_{j_1+1, j_2} \right] + \\ & \left[(1 - \delta_{j_1, j_2-1}) W_{j_1, j_2-1} + (1 - \delta_{j_1, j_2+1}) W_{j_1, j_2+1} \right] \approx \\ & \approx E_{q_{j_1}+q_{j_2}}^{(K_{\uparrow}=2)} - \Delta_{q_{j_1}+q_{j_2}}^{zz}, \end{aligned} \quad (4.14)$$

where

$$\begin{aligned} \Delta_{q_{j_1}+q_{j_2}}^{zz} = & \left(\frac{\mathbf{h}}{2} - \sum_{k=1}^2 h_{j_k} \right) + J_z \left(\frac{K-1}{4} - 2 \right) \\ & + J_z \sum_{\ell=1}^2 g_{j_{\ell}} + J_z (\delta_{j_1, j_2+1} + \delta_{j_2, j_1+1}), \end{aligned} \quad (4.15)$$

and

$$W_{j_1, j_2 \pm 1} = \frac{\left(\frac{J}{2}\right)^2}{\Delta_{q_{j_1}+q_{j_2}}^{zz} - \Delta_{q_{j_1}+q_{j_2 \pm 1}}^{zz}}, \quad (4.16a)$$

$$W_{j_1 \pm 1, j_2} = \frac{\left(\frac{J}{2}\right)^2}{\Delta_{q_{j_1}+q_{j_2}}^{zz} - \Delta_{q_{j_1 \pm 1}+q_{j_2}}^{zz}}. \quad (4.16b)$$

Here,

$$\begin{aligned} \Delta_{q_{j_1}+q_{j_2}}^{zz} - \Delta_{q_{j_1 \pm 1}+q_{j_2}}^{zz} = & -(h_{j_1} - h_{j_1 \pm 1}) + J_z (g_{j_1} - g_{j_1 \pm 1}) \\ & + J_z (\delta_{j_1+1, j_2} - \delta_{j_1 \pm 2, j_2}), \end{aligned} \quad (4.17a)$$

$$\begin{aligned} \Delta_{q_{j_1}+q_{j_2}}^{zz} - \Delta_{q_{j_1}+q_{j_2 \pm 1}}^{zz} = & -(h_{j_2} - h_{j_2 \pm 1}) + J_z (g_{j_2} - g_{j_2 \pm 1}) \\ & + J_z (\delta_{j_1+1, j_2} - \delta_{j_1, j_2 \pm 2}). \end{aligned} \quad (4.17b)$$

Eq.(4.14) is subject to the constraint $W_{0, j_2} = W_{j_1, 0} = W_{j_1+K, j_2} = W_{j_1, j_2+K} = W_{j, j} = 0$. It mimics a two-dimensional semi-classical tight-binding model. Population transfer is equally done by successive jumps between neighboring states.

The energy in other sectors can be evaluated in a similar fashion. However, as suggested earlier, the perturbative energy being of the form (3.17), we have confirmed that in each sector it can be reduced to the tight-binding equation for P_j . For instance, (4.21) in the sector $K_{\uparrow} = 1$ mimics (3.20) while (4.14) mimics (3.28). It is then legitimate to claim without further calculations that in the sector $K_{\uparrow} = 3$ the energy will be of the form (3.38) with the respective constraints. Therefore, in arbitrary sector and without further evidence,

$$\begin{aligned} E_{q_{j_1}+q_{j_2}+\dots+q_{j_{K_{\uparrow}}}}^{(K_{\uparrow})} \approx & \Delta_{q_{j_1}+q_{j_2}+\dots+q_{j_{K_{\uparrow}}}}^{zz} + \\ & + \sum_{\ell=1}^{K_{\uparrow}} \left(\mathcal{X}_{j_{\ell}-1} W_{j_1, \dots, j_{\ell-1}, \dots, j_{K_{\uparrow}}} + \mathcal{X}_{j_{\ell}+1} W_{j_1, \dots, j_{\ell+1}, \dots, j_{K_{\uparrow}}} \right), \end{aligned} \quad (4.18)$$

where

$$W_{j_1, \dots, j_{\ell \pm 1}, \dots, j_{K_{\uparrow}}} = \frac{\left(\frac{J}{2}\right)^2}{\Delta_{q_{j_1}+q_{j_2}+\dots+q_{j_{K_{\uparrow}}}}^{zz} - \Delta_{q_{j_1}+q_{j_2}+\dots+q_{j_{\ell \pm 1}}+q_{j_{\ell+1}}+\dots+q_{j_{K_{\uparrow}}}}^{zz}}. \quad (4.19)$$

The constraints on the $W_{j_1, \dots, j_\ell \pm 1, \dots, j_K}$ are the same as those on P_{j_ℓ, \dots, j_K} . The denominator of (4.19) are calculated from (4.10).

2. Eigenstates

For the eigenstates, after calculations one obtains at the first order,

$$|\psi_n^{(1)}\rangle = \sum_{j=1}^{K-1} \left(\frac{\Delta_n^{(j)+}}{\Lambda_{n,n+Q_j}} |n+Q_j\rangle + \frac{\Delta_n^{(j)-}}{\Lambda_{n,n-Q_j}} |n-Q_j\rangle \right). \quad (4.20)$$

This relation is also of the form (3.17). Thus, without further calculations and for the same reasons as evoked earlier, it can be broken down into sectors exactly as we did for the energies. In the second and third sectors for example:

$$|\psi_{q_j}\rangle \approx |q_j\rangle + (W_{j,j+1}|q_{j+1}\rangle + W_{j,j-1}|q_{j-1}\rangle). \quad (4.21)$$

and

$$\begin{aligned} |\psi_{q_{j_1}+q_{j_2}}\rangle &\approx |q_{j_1}+q_{j_2}\rangle + \left[(1-\delta_{j_1-1,j_2}) W_{j_1-1,j_2} |q_{j_1-1}+q_{j_2}\rangle \right. \\ &\quad + (1-\delta_{j_1+1,j_2}) W_{j_1+1,j_2} |q_{j_1+1}+q_{j_2}\rangle \Big] \\ &\quad + \left[(1-\delta_{j_1,j_2-1}) W_{j_1,j_2-1} |q_{j_1}+q_{j_2-1}\rangle \right. \\ &\quad \left. + (1-\delta_{j_1,j_2+1}) W_{j_1,j_2+1} |q_{j_1}+q_{j_2+1}\rangle \right]. \end{aligned} \quad (4.22)$$

The second order correction can be calculated in a similar manner and broken into sectors. This task is left for future projects.

We learn from (4.21) that if h_i and h_j strongly varies while J_z is maintained constant and small compared to the difference $h_i - h_j$, the denominator of $W_{i,j}$ can be very small leading it to acquiring large values while it remains small at other sites. This distorts the wave function causing it to concentrate in certain regions, effectively localizing the states. If the h_i smoothly vary, the eigenstates remain extended but may exhibit weak localization effects.

The above perturbation theory holds for $|J| < 1$ and arbitrary J_z and local magnetic field. The regime $|J| \gg 1$ can be addressed by rotating \hat{H}_0 into the eigenbasis of \hat{H}_1 . In this case \hat{H}_1 becomes diagonal with elements the eigenvalues in (3.48) and the eigenstates (3.49). \hat{H}_0 now is off-diagonal and the exact above same calculations are repeated by replacing $|n\rangle \rightarrow |\psi_n\rangle$ and $\Delta_n^{zz} \rightarrow E_n$.

V. OUTLOOK AND PERSPECTIVE: SPIN-1 CASE

We have presented in previous Sections the “bra-ket” (Dirac representation) for spin-1/2 lattice operators and

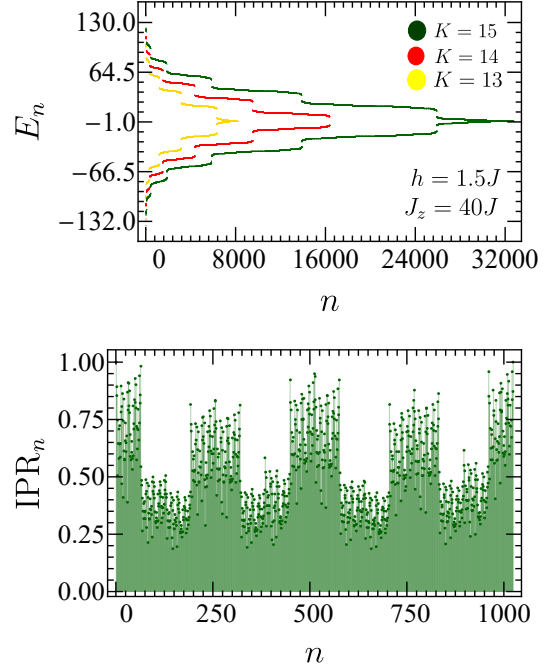


Figure 7. **Upper panel:** Energy of the model (3.1) as a function of n for various values of K . It has two branches consisting of cluster. Each cluster corresponds to a given value of the total magnetization. For even number K of spins, the branch $E_n > 0$ corresponds to the sectors $K/2 \leq J^z \leq 0$ while the branch $E_n < 0$ corresponds to the sectors $-K/2 \leq J^z < 0$. We observe that E_n increases with K . **Lower panel:** average inverse participation ratio, $IPR_n = \frac{1}{M} \sum_{r=1}^M |\psi_n^r|^4$ as a function of n for $M = 500$ realizations. ψ_n^r is the wave function after the r realization.

discussed a few applications. Because the case of spin-1 follows exactly the same logic, we found opportune to present it in this paper. In order to avoid lenghtly paper, possible applications are deferred to future projects.

In this case, spin projection along the quantization axis takes three values $+1, 0, -1$. These form qutrits the building blocks of ternary quantum computing. They are known to be robust against external unwanted nuisances, encoding more information (already at room temperature) compare to qubits and offering better security during communication[62, 63]. For these reasons it would be crucial to achieve qutrit without ternary decomposition as we did for qubits. This could improve on encrypting information during communications between quantum devices.

Foremost, note that qutrits can also be mapped onto their classical analogue $\sigma_n^{(j)} = \{0, 1, 2\}$ (the trits), of the base-3. Classical trits cannot be subjected to the principle of quantum superposition nor entanglement in contrast to their quantum analogue. Here, n is the positive integer whose decomposition in base 3 encapsulates the exact configuration of the projections $+1, 0, -1$. It

can exactly be written as in Eq.(2.7) now with $q_j = 3^K$ and $D = 3^K$. Without loss of generality, it can be assumed that $|+1\rangle \rightarrow |0\rangle = [1, 0, 0]^T$, $|0\rangle \rightarrow |1\rangle = [0, 1, 0]^T$ and $| -1\rangle \rightarrow |2\rangle = [0, 0, 1]^T$ yielding,

$$\langle m|S_j^x|n\rangle = \frac{1}{\sqrt{2}} \begin{cases} \delta_{m,\chi_j^{[n,1]}} , & \text{if } \sigma_n^{(j)} = 0, \\ \delta_{m,\chi_j^{[n,0]} + \delta_{m,\chi_j^{[n,2]}}} , & \text{if } \sigma_n^{(j)} = 1, \\ \delta_{m,\chi_j^{[n,1]}} , & \text{if } \sigma_n^{(j)} = 2, \end{cases} \quad (5.1)$$

$$\langle m|S_j^y|n\rangle = -\frac{i}{\sqrt{2}} \begin{cases} -\delta_{m,\chi_j^{[n,1]}} , & \text{if } \sigma_n^{(j)} = 0, \\ \delta_{m,\chi_j^{[n,0]} - \delta_{m,\chi_j^{[n,2]}}} , & \text{if } \sigma_n^{(j)} = 1, \\ \delta_{m,\chi_j^{[n,1]}} , & \text{if } \sigma_n^{(j)} = 2, \end{cases} \quad (5.2)$$

Here, the integer $\chi_j^{[n,a]}$ is the number obtained from the ternary decomposition of n by replacing the j th digit by a . For the same reasons as for the spin-1/2 case, we see that if $\sigma_n^{(j)} = 0$ then replacing this digit by 1 is equivalent to adding q_j . Similarly, if $\sigma_n^{(j)} = 1$ then replacing this digit by 0 or 2 is equivalent to subtracting q_j or adding q_j respectively. These observations can be translated in a mathematical language as

$$\chi_j^{[n,0]} = \begin{cases} n, & \text{if } \sigma_n^{(j)} = 0, \\ n + q_j, & \text{if } \sigma_n^{(j)} = 1, \\ n + 2q_j, & \text{if } \sigma_n^{(j)} = 2, \end{cases} \quad (5.3)$$

$$\chi_j^{[n,1]} = \begin{cases} n + q_j, & \text{if } \sigma_n^{(j)} = 0, \\ n, & \text{if } \sigma_n^{(j)} = 1, \\ n - q_j, & \text{if } \sigma_n^{(j)} = 2, \end{cases} \quad (5.4)$$

$$\chi_j^{[n,2]} = \begin{cases} n + 2q_j, & \text{if } \sigma_n^{(j)} = 0, \\ n - q_j, & \text{if } \sigma_n^{(j)} = 1, \\ n, & \text{if } \sigma_n^{(j)} = 2, \end{cases} \quad (5.5)$$

These functions are defined in the same philosophy as the **flip()** function in the spin-1/2 case. The promised Dirac notations are constructed from Eqs.(5.1) and (5.2) considering Eqs.(5.3)-(5.5). After considerable calculations one obtains

$$\hat{S}_j^+ = \sqrt{2} \sum_{n=0}^{D-1} \Gamma_n^{(j)+} |n - q_j\rangle \langle n|, \quad (5.6a)$$

$$\hat{S}_j^- = \sqrt{2} \sum_{n=0}^{D-1} \Gamma_n^{(j)-} |n + q_j\rangle \langle n|, \quad (5.6b)$$

$$\hat{S}_j^z = \sum_{n=0}^{D-1} \Gamma_n^{(j)z} |n\rangle \langle n|. \quad (5.6c)$$

Although a qutrit can exist in three distinct quantum states, we observe that apart from the $\sqrt{2}$ factor Eqs.(5.6) have the same structure as Eqs.(2.12) where now we have defined the classical trit,

$$\Gamma_n^{(j)+} = \delta\left(\sigma_n^{(j)}, 1\right) + \delta\left(\sigma_n^{(j)}, 2\right), \quad (5.7a)$$

$$\Gamma_n^{(j)-} = \delta\left(\sigma_n^{(j)}, 0\right) + \delta\left(\sigma_n^{(j)}, 1\right), \quad (5.7b)$$

$$\Gamma_n^{(j)z} = \delta\left(\sigma_n^{(j)}, 0\right) - \delta\left(\sigma_n^{(j)}, 2\right). \quad (5.7c)$$

Here, we have adopted the notation $\delta(n, m) \equiv \delta_{n,m}$. For all possible values of trits, it can be verified that

$$\Gamma_n^{(j)z} = \begin{cases} +1, & \text{if } \sigma_n^{(j)} = 0, \\ 0, & \text{if } \sigma_n^{(j)} = 1, \\ -1, & \text{if } \sigma_n^{(j)} = 2. \end{cases} \quad (5.8)$$

For the same reason as in the spin-1/2 case, our task at this point is incompletely completed. Despite the level of complexity has increased with S , we have equally disproved the idea that the value of a classical trit at a given location in the ternary representation of a positive integer can only be accessed with aid of a computer. We have conducted a very same experiment as earlier (see Appendix.A). Deep inspection into the nature of digits in a few numbers brought us to the conclusion that classical trits also enter numbers through specific patterns similar to those for bits (see Fig.1). The trits are also constructed in terms of the unit-step function as

$$\Gamma_n^{(j)+} = \sum_{m=0}^{r_{j-1}-1} \left(u(n - (3m+1)q_j) - u(n - (3m+3)q_j) \right) \quad (5.9a)$$

$$\Gamma_n^{(j)-} = \sum_{m=0}^{r_{j-1}-1} \left(u(n - 3mq_j) - u(n - (3m+2)q_j) \right), \quad (5.9b)$$

$$\begin{aligned} \Gamma_n^{(j)z} = & \sum_{m=0}^{r_{j-1}-1} \left(u(n - 3mq_j) - u(n - (3m+1)q_j) \right) \\ & - \sum_{m=0}^{r_{j-1}-1} \left(u(n - (3m+2)q_j) - u(n - (3m+3)q_j) \right) \end{aligned} \quad (5.9c)$$

with $r_j = 3^j$. It can be verified that $\Gamma_n^{(j)-} - \Gamma_n^{(j)+} = \Gamma_n^{(j)z}$ and that the following conjugation relations $\Gamma_{n+q_j}^{(j)+} = \Gamma_n^{(j)-}$ and $\Gamma_{n-q_j}^{(j)-} = \Gamma_n^{(j)+}$ hold. At this stage, a key question pop up in mind: can we extend this technique to $S > 1$? The answer is affirmative as it is always possible to map quantum spins of size $S > 1$ (qudits) onto their classical counterpart. As a consequence the d -decomposition in d -trit basis yields exactly the configuration of the d -spin. In the general case $q_j = (2S+1)^{K-j}$ and $r_j = (2S+1)^j$ (this tasks is left for future projects).

VI. CONCLUSION

We have considered the fundamental problem of achieving suitable representations for lattice spin operators (LSOs) without any drawback. Due to its inherent *abstract algebra* that alleviates manipulating quantum objects, Dirac representations are highly desired in Physics. So far, in spin systems this has been achieved only for spin-1/2 and spin-1 Pauli matrices (one-particle spin system). That is, for more than one particle no such representation is known. We believe we have filled this gap for spin-1/2 and spin-1 LSOs thanks to a profound binary/ternary analysis. We also believe that our results have potential for improvement not just in physics but broadly in science as they offer the possibility of getting the j th bit/trit of an integer of bit/trit -field length K without resorting to a binary/ternary decomposition. The usefulness of our representations are discussed in Physics by revisiting the spin-1/2 XXZ Heisenberg model in an open boundary configuration in a magnetic field. Two complementary limits of the magnetic field are considered: the case of uniform and random magnetic field. In the first case, the prototype model is analyzed both numerically and analytically. We have found that binary representation allows a rapid construction of the Hamiltonian by avoiding costly matrix matrix multiplication. The global $U(1)$ symmetry is exploited permitting alleviating finite-size effects due to the exponential growth of the Hilbert space with the total number of spins. The spin-inversion symmetry is also exploited to once again reduce the finite-size effects in the sector with total magnetization $\mathcal{J}^z = 0$ and in the absence of local magnetic field. Thus, on a 32Gb computer we have been able to implement up to $K = 18$ spins on Mathematica 7. Algorithms and programs are available in the [GitHub repository](#). For analytical treatment, the eigenvalues equation is reduced to a recurrence equation. We turned off a first time the anisotropy parameter ($J_z = 0$) for simplicity and transform the previous equation into multi-dimensional tight-binding equation that can easily be solved. In a second time, we turn it on and addressed the full model with random magnetic field perturbatively. Expressions for the eigenenergies and eigenvectors are derived and compared with data from exact diagonalization. A nice agreement between both data is reported.

Although a few successes can already be ascribed to our representation, a few questions asked in this paper are left here without technical answers and for future projects. For example, IPR is calculated but not discussed in details, clustering of nearly-degenerate energies in the presence of disorder is not explained, consequences of having E_{q_j} in explicit form on MBL is partially addressed. Our main goal was to pave a way to understanding a broad range of phenomena. It will be interesting in the future to inspect whether our technique applies to long-range interactions and not necessarily nearest-neighbor interactions and whether these

are extensible to higher dimensions. It would also be interesting to investigate the possibility of achieving a Dirac representation for Boson operators on lattices.

ACKNOWLEDGMENTS

This paper is part of the project “Building a Comprehensive Quantum Theory for Many-Body Localization in Spin chains.” Fundings for this paper are provided by the Alexander von Humboldt foundation through the scheme of Georg-Forster fellowship for Postdocs. MBK appreciates the warm hospitality of Prof. John Schliemann at the University of Regensburg where part of this paper was conducted.

Appendix A: Proof

This Appendix is devoted to proofing the formula (2.13a)-(2.13c). This is done by conducting the following experiment: Consider a chain of length K with identical spins of size $S = 1/2$. There exist 2^K different configurations (possible way of arranging spins in up-and/or down- directions). Mapping the quantum spins onto their classical analogue and sorting the basis vectors $|n\rangle$ in lexicographical order with respect to the site j , we construct the diagrams in Fig.8 for $K = \{3, 4, 5\}$. Blue and red colors are used to discriminate between possible orientations of spins along the quantization direction. With the aid of such a color palette the diagrams depict a clear pattern. This is clearly seen by standing on each site and looking at the numbers n . For instance, at site $j = 1$ for $K = 5$ (reading direction- from the left to the right), we observe that for all integer in the interval $0 \leq n \leq 15$ the first spin is in the state $\sigma_n^{(1)} = 0$ whilst for $16 \leq n \leq 32$ one always has $\sigma_n^{(1)} = 1$. Similarly, at site $j = 2$ all integers in the interval $0 \leq n \leq 7$ have $\sigma_n^{(2)} = 0$ those in $8 \leq n \leq 15$ have $\sigma_n^{(2)} = 1$ while those in $16 \leq n \leq 23$ have $\sigma_n^{(2)} = 1$ etc The same observation can be done at every site.

The very same experiment is repeated for $S = 1$ in order to prove (5.9a)-(5.9c).

1. Spin-1/2

The report concerning the above experiment for $K = 5$ is presented as follows. Other values of K in the diagram Fig.8 leading to the same conclusion.

At site $j = 1$,

$$\begin{aligned} 0 \cdot 2^{(5-1)} \leq n < 1 \cdot 2^{(5-1)}, \quad \sigma_n^{(1)} &= 0, \\ 1 \cdot 2^{(5-1)} \leq n < 2 \cdot 2^{(5-1)}, \quad \sigma_n^{(1)} &= 1. \end{aligned} \quad (\text{A1})$$

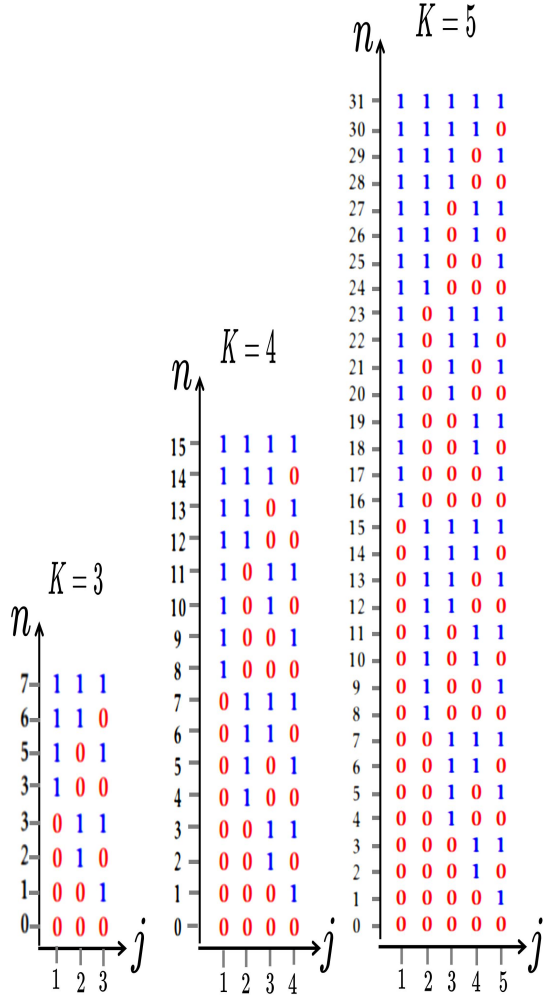


Figure 8. Binary decomposition of integers $0 \leq n \leq 2^K - 1$ for $K = \{3, 4, 5\}$ using color palette to distinguish between bits. We observe from these diagrams that $s_n^{(K)+} = 0$ for even integers n while $s_n^{(K)+} = 1$ for odd integers n .

At site $j = 2$,

$$\begin{aligned} 0 \cdot 2^{(5-2)} \leq n < 1 \cdot 2^{(5-2)}, \quad \sigma_n^{(2)} = 0, \\ 1 \cdot 2^{(5-2)} \leq n < 2 \cdot 2^{(5-2)}, \quad \sigma_n^{(2)} = 1, \\ 2 \cdot 2^{(5-2)} \leq n < 3 \cdot 2^{(5-2)}, \quad \sigma_n^{(2)} = 0, \\ 3 \cdot 2^{(5-2)} \leq n < 4 \cdot 2^{(5-2)}, \quad \sigma_n^{(2)} = 1. \end{aligned}$$

At site $j = 3$,

$$\begin{aligned} 0 \cdot 2^{(5-3)} \leq n < 1 \cdot 2^{(5-3)}, \quad \sigma_n^{(3)} = 0, \\ 1 \cdot 2^{(5-3)} \leq n < 2 \cdot 2^{(5-3)}, \quad \sigma_n^{(3)} = 1, \\ 2 \cdot 2^{(5-3)} \leq n < 3 \cdot 2^{(5-3)}, \quad \sigma_n^{(3)} = 0, \\ 3 \cdot 2^{(5-3)} \leq n < 4 \cdot 2^{(5-3)}, \quad \sigma_n^{(3)} = 1, \\ 4 \cdot 2^{(5-3)} \leq n < 5 \cdot 2^{(5-3)}, \quad \sigma_n^{(3)} = 0, \\ 5 \cdot 2^{(5-3)} \leq n < 6 \cdot 2^{(5-3)}, \quad \sigma_n^{(3)} = 1, \\ 6 \cdot 2^{(5-3)} \leq n < 7 \cdot 2^{(5-3)}, \quad \sigma_n^{(3)} = 0, \\ 7 \cdot 2^{(5-3)} \leq n < 8 \cdot 2^{(5-3)}, \quad \sigma_n^{(3)} = 1. \end{aligned} \quad (\text{A2})$$

At site $j = 4$,

$$\begin{aligned} 0 \cdot 2^{(5-4)} \leq n < 1 \cdot 2^{(5-4)}, \quad \sigma_n^{(4)} = 0, \\ 1 \cdot 2^{(5-4)} \leq n < 2 \cdot 2^{(5-4)}, \quad \sigma_n^{(4)} = 1, \\ 2 \cdot 2^{(5-4)} \leq n < 3 \cdot 2^{(5-4)}, \quad \sigma_n^{(4)} = 0, \\ 3 \cdot 2^{(5-4)} \leq n < 4 \cdot 2^{(5-4)}, \quad \sigma_n^{(4)} = 1, \\ &\vdots \\ 13 \cdot 2^{(5-4)} \leq n < 14 \cdot 2^{(5-4)}, \quad \sigma_n^{(4)} = 1, \\ 14 \cdot 2^{(5-4)} \leq n < 15 \cdot 2^{(5-4)}, \quad \sigma_n^{(4)} = 0, \\ 15 \cdot 2^{(5-4)} \leq n < 16 \cdot 2^{(5-4)}, \quad \sigma_n^{(4)} = 1. \end{aligned} \quad (\text{A3})$$

At site $j = 5$,

$$\begin{aligned} 0 \cdot 2^{(5-5)} \leq n < 1 \cdot 2^{(5-5)}, \quad \sigma_n^{(5)} = 0, \\ 1 \cdot 2^{(5-5)} \leq n < 2 \cdot 2^{(5-5)}, \quad \sigma_n^{(5)} = 1, \\ 2 \cdot 2^{(5-5)} \leq n < 3 \cdot 2^{(5-5)}, \quad \sigma_n^{(5)} = 0, \\ &\vdots \\ 29 \cdot 2^{(5-5)} \leq n < 30 \cdot 2^{(5-5)}, \quad \sigma_n^{(5)} = 1, \\ 30 \cdot 2^{(5-5)} \leq n < 31 \cdot 2^{(5-5)}, \quad \sigma_n^{(5)} = 0, \\ 31 \cdot 2^{(5-5)} \leq n < 32 \cdot 2^{(5-5)}, \quad \sigma_n^{(5)} = 1. \end{aligned} \quad (\text{A4})$$

By inspecting the structure of integers, we observe that all integers in an appropriately chosen interval have the same value of the j th digit as indicated in Table I below. From this table we easily infer (2.13a)-(2.13c) and achieve our goal.

In general, a given piece-wise function $f(n)$ defined as

$$f(n) = \begin{cases} n_1, & \text{if } a_1 \leq n < a_2 \\ n_2, & \text{if } a_2 \leq n < a_3 \\ n_3, & \text{if } a_3 \leq n < a_4 \\ & \vdots \\ n_L, & \text{if } a_{L-1} \leq n < a_L \end{cases} \quad (\text{A5})$$

can be written in terms of unit-step function $u(x)$ as

$$f(n) = \sum_{j=1}^{L-1} n_j [u(n - a_j) - u(n - a_{j+1})]. \quad (\text{A6})$$

Table I. Table of the values of classical spins in the range $0 \leq n \leq 2^K - 1$ splitted into $r_j = 2^j$ intervals with $q_j = 2^{K-j}$.

Intervals ($S = 1/2$)	$s_n^{(j)+}$	$s_n^{(j)-}$	$s_n^{(j)z}$
$0 \cdot q_j \leq n < 1 \cdot q_j$	0	1	$\frac{1}{2}$
$1 \cdot q_j \leq n < 2 \cdot q_j$	1	0	$-\frac{1}{2}$
$2 \cdot q_j \leq n \leq 3 \cdot q_j$	0	1	$\frac{1}{2}$
\vdots	\vdots	\vdots	\vdots
$(r_j - 2) \cdot q_j \leq n < (r_j - 1) \cdot q_j$	0	1	$\frac{1}{2}$
$(r_j - 1) \cdot q_j \leq n < (r_j - 0) \cdot q_j$	1	0	$-\frac{1}{2}$

Table II. Table of the binary decomposition of even integers in bit-field length $K = 4$ for numbers in the interval $0 \leq n \leq 2^K - 1$

even number, n	$j = 1$	$j = 2$	$J = 3$	$J = 4$
14	$-\frac{1}{2}$	$-\frac{1}{2}$	$-\frac{1}{2}$	$\frac{1}{2}$
12	$-\frac{1}{2}$	$-\frac{1}{2}$	$\frac{1}{2}$	$\frac{1}{2}$
10	$-\frac{1}{2}$	$\frac{1}{2}$	$-\frac{1}{2}$	$\frac{1}{2}$
8	$-\frac{1}{2}$	$\frac{1}{2}$	$\frac{1}{2}$	$\frac{1}{2}$
6	$\frac{1}{2}$	$-\frac{1}{2}$	$-\frac{1}{2}$	$\frac{1}{2}$
4	$\frac{1}{2}$	$-\frac{1}{2}$	$\frac{1}{2}$	$\frac{1}{2}$
2	$\frac{1}{2}$	$\frac{1}{2}$	$-\frac{1}{2}$	$\frac{1}{2}$
0	$\frac{1}{2}$	$\frac{1}{2}$	$\frac{1}{2}$	$\frac{1}{2}$

An interesting fact to be noted is that if we split the set of integers in the interval $0 \leq n \leq 2^K - 1$ into even and odd integers, perform binary decomposition, replace $0 \rightarrow \frac{1}{2}$ and $1 \rightarrow -\frac{1}{2}$, we observe that both results differ only by the least significant digit (LSD). This is illustrated for $K = 4$ in the Tables II and III. As mentioned in the main text, the LSD is the digit at $j = K$ as we have adopted the reading-coding direction – from the left to the right.

We observe that apart from last columns corresponding to least significant digits (LSDs), both Tables are identical. Same observations can be done for $K > 4$.

Table III. Same as Table II for odd integers.

odd number, n	$j = 1$	$j = 2$	$J = 3$	$J = 4$
15	$-\frac{1}{2}$	$-\frac{1}{2}$	$-\frac{1}{2}$	$-\frac{1}{2}$
13	$-\frac{1}{2}$	$-\frac{1}{2}$	$\frac{1}{2}$	$-\frac{1}{2}$
11	$-\frac{1}{2}$	$\frac{1}{2}$	$-\frac{1}{2}$	$-\frac{1}{2}$
9	$-\frac{1}{2}$	$\frac{1}{2}$	$\frac{1}{2}$	$-\frac{1}{2}$
7	$\frac{1}{2}$	$-\frac{1}{2}$	$-\frac{1}{2}$	$-\frac{1}{2}$
5	$\frac{1}{2}$	$-\frac{1}{2}$	$\frac{1}{2}$	$-\frac{1}{2}$
3	$\frac{1}{2}$	$\frac{1}{2}$	$-\frac{1}{2}$	$-\frac{1}{2}$
1	$\frac{1}{2}$	$\frac{1}{2}$	$\frac{1}{2}$	$-\frac{1}{2}$

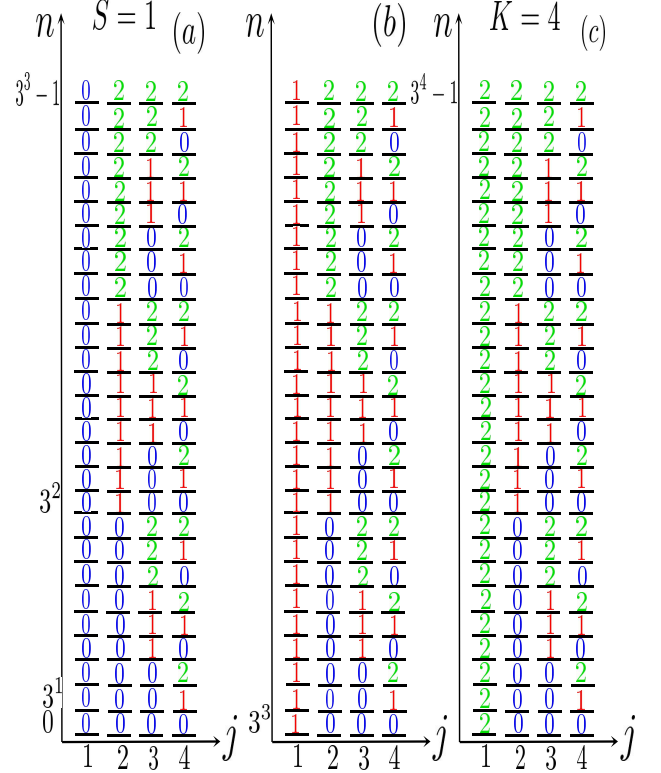


Figure 9. Same as 8 for $S = 1$.

This is clearly an indication that if one knows the binary decomposition of an odd/even number, one can infer the binary decomposition of the consecutive even/odd number just by flipping the LSD. For example the two consecutive digits 0 and 1 differ only by the last digits etc.

2. Spin-1

The report concerning the experiment for $S = 1$ and $K = 4$ is presented as follows:

At site $j = 1$,

$$\begin{aligned} 0 \cdot 3^{(4-1)} \leq n < 1 \cdot 3^{(4-1)}, \quad \sigma_n^{(1)} &= 0, \\ 1 \cdot 3^{(4-1)} \leq n < 2 \cdot 3^{(4-1)}, \quad \sigma_n^{(1)} &= 1, \\ 2 \cdot 3^{(4-1)} \leq n < 3 \cdot 3^{(4-1)}, \quad \sigma_n^{(1)} &= 2. \end{aligned} \quad (\text{A7})$$

At site $j = 2$,

$$\begin{aligned} 0 \cdot 3^{(4-2)} \leq n < 1 \cdot 3^{(4-2)}, \quad \sigma_n^{(2)} = 0, \\ 1 \cdot 3^{(4-2)} \leq n < 2 \cdot 3^{(4-2)}, \quad \sigma_n^{(2)} = 1, \\ 2 \cdot 3^{(4-2)} \leq n < 3 \cdot 3^{(4-2)}, \quad \sigma_n^{(2)} = 2, \\ \vdots & \\ 6 \cdot 3^{(4-2)} \leq n < 7 \cdot 3^{(4-2)}, \quad \sigma_n^{(2)} = 0, \\ 7 \cdot 3^{(4-2)} \leq n < 8 \cdot 3^{(4-2)}, \quad \sigma_n^{(2)} = 1, \\ 8 \cdot 3^{(4-2)} \leq n < 9 \cdot 3^{(4-2)}, \quad \sigma_n^{(2)} = 2. \end{aligned} \tag{A8}$$

At site $j = 3$,

$$\begin{aligned} 0 \cdot 3^{(4-3)} \leq n < 1 \cdot 3^{(4-3)}, \quad \sigma_n^{(3)} = 0, \\ 1 \cdot 3^{(4-3)} \leq n < 2 \cdot 3^{(4-3)}, \quad \sigma_n^{(3)} = 1, \\ 2 \cdot 3^{(4-3)} \leq n < 3 \cdot 3^{(4-3)}, \quad \sigma_n^{(3)} = 2, \\ \vdots & \\ 24 \cdot 3^{(4-3)} \leq n < 25 \cdot 3^{(4-3)}, \quad \sigma_n^{(3)} = 0, \\ 25 \cdot 3^{(4-3)} \leq n < 26 \cdot 3^{(4-3)}, \quad \sigma_n^{(3)} = 1, \\ 26 \cdot 3^{(4-3)} \leq n < 27 \cdot 3^{(4-3)}, \quad \sigma_n^{(3)} = 2. \end{aligned} \tag{A9}$$

At site $j = 4$,

$$\begin{aligned} 0 \cdot 3^{(4-4)} \leq n < 1 \cdot 3^{(4-4)}, \quad \sigma_n^{(4)} = 0, \\ 1 \cdot 3^{(4-4)} \leq n < 2 \cdot 3^{(4-4)}, \quad \sigma_n^{(4)} = 1, \\ 2 \cdot 3^{(4-4)} \leq n < 3 \cdot 3^{(4-4)}, \quad \sigma_n^{(4)} = 2, \\ \vdots & \\ 78 \cdot 3^{(4-4)} \leq n < 79 \cdot 3^{(4-4)}, \quad \sigma_n^{(4)} = 0, \\ 79 \cdot 3^{(4-4)} \leq n < 80 \cdot 3^{(4-4)}, \quad \sigma_n^{(4)} = 1, \\ 80 \cdot 3^{(4-4)} \leq n < 81 \cdot 3^{(4-4)}, \quad \sigma_n^{(4)} = 2. \end{aligned} \tag{A10}$$

Appendix B: A few properties of the classical spins

A few properties of classical spins-1/2 are elaborated and presented below:

$$\left(s_n^{(j)+}\right)^2 = s_n^{(j)+}, \quad \left(s_n^{(j)-}\right)^2 = s_n^{(j)-}, \quad \left(s_n^{(j)z}\right)^2 = \frac{1}{4}, \tag{B1}$$

$$s_n^{(j)+} s_n^{(j)-} = s_n^{(j)-} s_n^{(j)+} = 0, \tag{B2a}$$

$$s_n^{(j)+} s_n^{(j)z} = -\frac{s_n^{(j)+}}{2}, \tag{B3a}$$

$$s_n^{(j)-} s_n^{(j)z} = \frac{s_n^{(j)-}}{2}, \tag{B4a}$$

Table IV. Table of the values of classical spins in the range $0 \leq n \leq 3^K - 1$ splitted into $r_j = 3^j$ intervals with $q_j = 3^{K-j}$.

Intervals ($S = 1$)	$\Gamma_n^{(j)+}$	$\Gamma_n^{(j)-}$	$\Gamma_n^{(j)z}$
$0 \cdot q_j \leq n < 1 \cdot q_j$	0	1	1
$1 \cdot q_j \leq n < 2 \cdot q_j$	1	1	0
$2 \cdot q_j \leq n < 3 \cdot q_j$	1	0	-1
$3 \cdot q_j \leq n < 4 \cdot q_j$	0	1	1
$4 \cdot q_j \leq n < 5 \cdot q_j$	1	1	0
$5 \cdot q_j \leq n < 6 \cdot q_j$	1	0	-1
\vdots	\vdots	\vdots	\vdots
$(r_j - 3) \cdot q_j \leq n < (r_j - 2) \cdot q_j$	0	1	1
$(r_j - 2) \cdot q_j \leq n < (r_j - 1) \cdot q_j$	1	1	0
$(r_j - 1) \cdot q_j \leq n < (r_j - 0) \cdot q_j$	1	0	-1

and

$$s_n^{(j)+} + s_n^{(j)-} = 1, \quad s_n^{(j)+} - s_n^{(j)-} = -2s_n^{(j)z}, \tag{B5}$$

whereby

$$s_n^{(j)z} = \frac{1}{2} \left(1 - 2s_n^{(j)+} \right) = -\frac{1}{2} \left(1 - 2s_n^{(j)-} \right), \tag{B6}$$

$$s_n^{(j)+} = \frac{1}{2} \left(1 - 2s_n^{(j)z} \right), \quad s_n^{(j)-} = \frac{1}{2} \left(1 + 2s_n^{(j)z} \right). \tag{B7}$$

As a consequence of these first properties $\cos(\alpha s_n^{(j)\pm}) = s_n^{(j)\mp} + s_n^{(j)\pm} \cos(\alpha) = 1 - 2s_n^{(j)\pm} \sin^2(\alpha/2)$ and $\sin(\alpha s_n^{(j)\pm}) = s_n^{(j)\pm} \sin(\alpha)$. When the angle $\alpha = \pi/2$ then $\cos(\pi s_n^{(j)\pm}/2) = 1 - 2s_n^{(j)\pm}$ and $\sin(\pi s_n^{(j)\pm}/2) = s_n^{(j)\pm}$ thereby $s_n^{(j)z} = \frac{1}{2} \cos(\pi s_n^{(j)\pm}/2)$. In the same vein, one easily proves that $\cos(\pi s_n^{(j)z}) = 0$ and $\sin(\pi s_n^{(j)z}) = 2s_n^{(j)z}$. From Eqs.(2.13a)-(2.13c) we have also verified the relations

$$s_{n+q_j}^{(j)+} = s_n^{(j)-}, \quad s_{n-q_j}^{(j)-} = s_n^{(j)+}, \tag{B8a}$$

$$s_{n+q_j}^{(j)+} = s_n^{(j)-}, \quad s_{n-q_j}^{(j)-} = s_n^{(j)+}, \tag{B8b}$$

$$s_{D-1-n}^{(j)+} = s_n^{(j)-}, \quad s_{D-1-n}^{(j)-} = s_n^{(j)+}, \tag{B8c}$$

$$s_{D-1-n}^{(j)+} = s_n^{(j)-}, \quad s_{D-1-n}^{(j)-} = s_n^{(j)+}, \tag{B8d}$$

$$s_{D-1-n-q_j}^{(j)-} = s_{n+q_j}^{(j)+} = s_n^{(j)-}, \quad s_{D-1-n+q_j}^{(j)+} = s_{n-q_j}^{(j)-} = s_n^{(j)+} \tag{B8e}$$

Thereby, for $0 \leq n \leq 2^K - 1$

$$s_{n+q_j}^{(j)z} = -s_n^{(j)z}, \tag{B9}$$

$$s_{D-1-n}^{(j)z} = -s_n^{(j)z}, \tag{B10}$$

and for $n \geq q_j$

$$s_{n-q_j}^{(j)z} = -s_n^{(j)z}, \quad (\text{B11})$$

confirming that the states $|n \pm q_j\rangle$ correspond to $|n\rangle$ with a flipped j th spin.

$$s_n^{(j)+} s_n^{(j+1)-} s_n^{(j)z} s_n^{(j+1)z} = -\frac{1}{4} s_n^{(j)+} s_n^{(j+1)-}, \quad (\text{B12a})$$

$$s_n^{(j)-} s_n^{(j+1)+} s_n^{(j)z} s_n^{(j+1)z} = -\frac{1}{4} s_n^{(j)-} s_n^{(j+1)+}. \quad (\text{B13a})$$

Similarly,

$$s_{n \pm m}^{(j)+} = s_n^{(j)+} \pm s_m^{(j)+}. \quad (\text{B14})$$

Eq.(2.12) must preserve the $su(2)$ algebra. The following properties are of importance: $\langle n|m + q_j\rangle = \langle n - q_j|m\rangle$ and $\langle n \pm q_j|m \pm q_j\rangle = \langle n|m\rangle$. Demanding that Eq.(2.12) preserves the $su(2)$ algebra allows to infer the following properties

$$s_{n+q_j}^{(j)+} s_n^{(j)-} - s_{n+q_j}^{(j)-} s_n^{(j)+} = 2s_n^{(j)z}, \quad (\text{B15a})$$

$$s_{n-q_j}^{(j)z} s_n^{(j)+} - s_n^{(j)+} s_n^{(j)z} = s_n^{(j)+}, \quad (\text{B15b})$$

$$s_{n+q_j}^{(j)z} s_n^{(j)-} - s_n^{(j)-} s_n^{(j)z} = -s_n^{(j)-}. \quad (\text{B15c})$$

These last relations can be verified with aid of previous relations. It can also be demonstrated that

$$s_{n+Q_j}^{(j)+} = s_{n-Q_j}^{(j)-}, \quad n \geq q_{j+1} \quad (\text{B16})$$

and that

$$s_{n-Q_j}^{(j)+} s_n^{(j)+} = s_{n+Q_j}^{(j)-} s_n^{(j)-} = 0, \quad (\text{B17a})$$

$$s_{n+Q_j}^{(j)+} s_n^{(j+1)-} = s_n^{(j)+} s_n^{(j+1)-}, \quad (\text{B17b})$$

$$s_{n-Q_j}^{(j)-} s_n^{(j+1)+} = s_n^{(j)-} s_n^{(j+1)+}. \quad (\text{B17c})$$

The following identities can easily be verified:

$$\sum_{j=1}^K \sum_{m=0}^{r_{j-1}-1} [u(n - 2mq_j) - u(n - (2m+1)q_j)] q_j = n, \quad (\text{B18})$$

$$\sum_{j=1}^K \sum_{m=0}^{r_j-2} [u(n - 2mq_j) - u(n - (2m-2)q_j)] = K, \quad (\text{B19})$$

$$\sum_{m=0}^{r_j-2} [u(n - 2mq_j) - u(n - (2m-2)q_j)] = 1, \quad (\text{B20})$$

$$\sum_{j=1}^K \sum_{m=0}^{r_j-2} [u(n - 2mq_j) - u(n - (2m-2)q_j)] q_j = 2^K - 1, \quad (\text{B21})$$

$$\sum_{j=1}^K \sum_{m=0}^{r_j-1} (-1)^m [u(n - mq_j) - u(n - (m+1)q_j)] = m_n^z, \quad (\text{B22})$$

where m_n^z is the n th magnetization quantum number.

Appendix C: Perturbation theory

According to the traditional perturbation theory, the eigenvalues and eigenstates of a partitioned Hamiltonian $\hat{H} = \hat{\Lambda} + \lambda \hat{\Delta}$ with $\hat{\Lambda}$ a diagonal matrix in the original Hilbert space and $\hat{\Delta}$ an off-diagonal matrix obeying $\hat{H}|\psi_n\rangle = E_n|\psi_n\rangle$ can be constructed as (see Ref.[64])

$$E_n = \sum_{k=0}^{\mathcal{K}} \lambda^k \mathcal{E}_n^{(k)} = \epsilon_n + \sum_{k=1}^{\mathcal{K}} \lambda^k \mathcal{E}_n^{(k)}, \quad (\text{C1})$$

and

$$|\psi_n\rangle = \sum_{k=0}^{\mathcal{K}} \lambda^k |\psi_n^{(k)}\rangle = |n\rangle + \sum_{k=1}^{\mathcal{K}} \lambda^k |\psi_n^{(k)}\rangle, \quad (\text{C2})$$

where $\hat{\Lambda}|n\rangle = \epsilon_n|n\rangle$ with \mathcal{K} the order of the correction. Here, $\mathcal{E}_n^{(k)}$ and $|\psi_n^{(k)}\rangle$ are respectively the k th order corrections to the energy and wave function. Plugging Eqs.(C1) and (C2) into the eigenvalue equation,

$$\sum_{k=0}^{\infty} \lambda^k (\hat{\Lambda} + \lambda \hat{\Delta}) |\psi_n^{(k)}\rangle = \left(\sum_{k=0}^{\infty} \lambda^k \mathcal{E}_n^{(k)} \right) \left(\sum_{k=0}^{\infty} \lambda^k |\psi_n^{(k)}\rangle \right). \quad (\text{C3})$$

The product of power series in the above equation is reduced to a single power series with aid of the Cauchy product formula. Comparing the left and right hand sides of the resulting equation leads for $k = 0$ to $\hat{\Delta}|\psi_n^{(0)}\rangle = \mathcal{E}_n^{(0)}|\psi_n^{(0)}\rangle$ and,

$$(\hat{\Lambda} - \mathcal{E}_n^{(0)} \mathbb{I}) |\psi_n^{(k)}\rangle = \sum_{q=1}^k \mathcal{E}_n^{(q)} |\psi_n^{(k-q)}\rangle - \hat{\Delta} |\psi_n^{(k-1)}\rangle, \quad k \geq 1. \quad (\text{C4})$$

We immediately infer from here that $\mathcal{E}_n^{(0)} = \epsilon_n$ and $|\psi_n^{(0)}\rangle = |n\rangle$. Eq.(C4) is further transformed by expanding the correction $|\psi_n^{(k)}\rangle$ into the eigenbasis of $\hat{\Lambda}$ as

$$|\psi_n^{(k)}\rangle = \sum_{j=1}^D A_{j,n}^{(k)} |j\rangle. \quad (\text{C5})$$

We observe that the coefficients $A_{j,n}^{(k)}$ of the expansion fully determine the wave function. We show below that they also determine the eigenenergies. Before coming to their evaluation, let us establish a few

properties. We note from $|\psi_n^{(0)}\rangle = |n\rangle$ that $A_{j,n}^{(0)} = \delta_{j,n}$ (which we name as condition (i)). For normalized wave functions, the requirement $\langle\psi_n|\psi_n\rangle = 1$ also reads $\sum_{k,k'=0}^{\infty} \lambda^{k+k'} \langle\psi_n^{(k)}|\psi_n^{(k')}\rangle = 1$. However, this requirement is met for $k = k' = 0$, therefore, $\sum_{k+k' \geq 1}^{\infty} \lambda^{k+k'} \langle\psi_n^{(k)}|\psi_n^{(k')}\rangle = 0$. Given that the scalar products $\langle\psi_n^{(k)}|\psi_n^{(k')}\rangle$ are defined to be all positive, we infer that $\langle\psi_n^{(k)}|\psi_n^{(k')}\rangle = 0$ for $k + k' \geq 1$. Eq.(C5) teaches us that $\sum_{j=1}^D A_{j,n}^{(k')} A_{j,n}^{(k)} = 0$ for $k + k' \geq 1$. By setting $k' = 0$ in the previous relation, we obtain $\sum_{j=1}^D \delta_{j,n} A_{j,n}^{(k)} = 0$ i.e. $A_{n,n}^{(k)} = 0$ (condition (ii)) which we combine with condition (i) to obtain the important relation $A_{n,n}^{(k)} = \delta_{k,0}$ (condition (iii)).

We can now construct the equation for the coefficients $A_{j,n}^{(k)}$. This is done by substituting (C5) into (C4) and sandwiching the resulting equation from the left with $\langle i|$. This recipe leads us to

$$A_{i,n}^{(k)} \left(\mathcal{E}_i^{(0)} - \mathcal{E}_n^{(0)} \right) = \sum_{q=1}^k \mathcal{E}_n^{(q)} A_{i,n}^{(k-q)} - \sum_{j=1}^D A_{j,n}^{(k-1)} \hat{\Delta}_{i,j}, \quad (\text{C6})$$

where $\hat{\Delta}_{i,j} = \langle i|\hat{\Delta}|j\rangle$. As mentioned earlier, the coefficients $A_{j,n}^{(k)}$ in this equation fully determine the eigenvalues as well. Indeed, setting $i = n$ and considering condition (iii) elaborated above readily yields,

$$\mathcal{E}_n^{(k)} = \sum_{j=1}^D A_{j,n}^{(k-1)} \hat{\Delta}_{n,j} = (\hat{\Delta} A^{(k-1)})_{n,n}. \quad (\text{C7})$$

Plugging this back into (C6) followed by a few manipulations and finally changing $i \rightarrow j$ leads us to

$$A_{j,n}^{(k)} = \vartheta_{j,n} \left(\sum_{q=1}^k (\hat{\Delta} A^{(q-1)})_{n,n} A_{j,n}^{(k-q)} - (\hat{\Delta} A^{(k-1)})_{j,n} \right), \quad (\text{C8})$$

where we have defined the matrix ϑ with matrix ele-

ments

$$\vartheta_{j,n} = \left(\mathcal{E}_j^{(0)} - \mathcal{E}_n^{(0)} \right)^{-1}, \quad \vartheta_{j,j} = 0. \quad (\text{C9})$$

Let us denote as $A^{(k)}$ a matrix whose entries are the covetted coefficients. Further inspection of Eq.(C8) reveals that the former obeys the matrix fixed-point equation,

$$A^{(k)} = \vartheta \circ \left(\sum_{q=1}^k A^{(k-q)} \mathcal{D}(\hat{\Delta} A^{(q-1)}) - (\hat{\Delta} A^{(k-1)}) \right). \quad (\text{C10})$$

Here, the symbol \circ denotes the elements-wise product operator (Hadamard product[65]). We have defined the operator $\mathcal{D}(X)$ which kills all off-diagonal elements of X i.e. the (ℓ, n) element resulting from its action on a matrix X reads $\mathcal{D}(X)_{\ell,n} = \delta_{\ell,n} X_{\ell,n}$. The eigenvalues and eigenstates are obtained from Eq.(C10) as

$$E_n = \epsilon_n + \sum_{j=1}^D \hat{\Delta}_{n,j} \left(\sum_{k=1}^{\infty} \lambda^k A_{j,n}^{(k)} \right) = \epsilon_n + \sum_{k=1}^{\infty} \lambda^k (\hat{\Delta} A^{(k-1)})_{n,n}, \quad (\text{C11})$$

$$|\psi_n\rangle = |n\rangle + \sum_{j=1}^D \left(\sum_{k=1}^{\infty} \lambda^k A_{j,n}^{(k-1)} \right) |j\rangle. \quad (\text{C12})$$

For example,

$$A^{(1)} = -(\vartheta \circ \hat{\Delta}), \quad (\text{C13})$$

$$A^{(2)} = -\vartheta \circ (\mathcal{D}(\hat{\Delta}(\vartheta \circ \hat{\Delta})) - \hat{\Delta}(\vartheta \circ \hat{\Delta})). \quad (\text{C14})$$

These formula are used to build the perturbation theory for random magnetic fields in the main text.

-
- [1] P. Dirac, A new notation for quantum mechanics, *Mathematical Proceedings of the Cambridge Philosophical Society*, **35**(3), 416-418 (1939).
 - [2] E. P and J. P, über das paulische äquivalenzverbot, *Zeitschrift für Physik* **5** (1928).
 - [3] T. Holstein and H. Primakoff, Field dependence of the intrinsic domain magnetization of a ferromagnet, *Phys. Rev.* **58**, 1098 (1940).
 - [4] J. Schwinger, On angular momentum [10.2172/4389568](https://doi.org/10.2172/4389568) (1952).
 - [5] F. J. Dyson, General theory of spin-wave interactions, *Phys. Rev.* **102**, 1217 (1956).
 - [6] S. V. Maleev, Scattering of slow neutrons in ferromagnets, *J. Exptl. Theoret. Phys.* **33**, 1010 (1957).
 - [7] M. N. Kiselev and R. Oppermann, Schwinger-keldysh semionic approach for quantum spin systems, *Phys. Rev. Lett.* **85**, 5631 (2000).
 - [8] M. Kiselev, H. Feldmann, and R. Oppermann, Semifermionic representation of su(n) hamiltonians, *The European Physical Journal B - Condensed Matter and Complex Systems* **22**, [10.1007/PL00011135](https://doi.org/10.1007/PL00011135) (2001).
 - [9] C. Herring and C. Kittel, On the theory of spin waves in ferromagnetic media, *Phys. Rev.* **81**, 869 (1951).
 - [10] A. Auerbach, Spin wave theory, in *Interacting Electrons and Quantum Magnetism* (Springer New York, New York, NY, 1994) pp. 113–127.
 - [11] M. Plihal, D. L. Mills, and J. Kirschner, Spin wave signature in the spin polarized electron energy loss spectrum

- of ultrathin fe films: Theory and experiment, *Phys. Rev. Lett.* **82**, 2579 (1999).
- [12] Locality in this context refers to how the transformations affect the spin representation in terms of fermionic and bosonic variable and thei spatial relation in the lattice. this is further clarified in the main text., () .
- [13] A. Abrikosov, L. Gorkov, I. Dzyaloshinski, and R. Silberman, *Methods of Quantum Field Theory in Statistical Physics*, Dover Books on Physics (Dover Publications, 2012).
- [14] V. N. Maleev and S. A. Fedotov, The functional-integration method and diagram technique for spin systems, *J. Exptl. Theoret. Phys.* **67**, 535 (1987).
- [15] O. Veits, R. Oppermann, M. Binderberger, and J. Stein, Extension of the popov-fedotov method to arbitrary spin, *J. Phys. I France* **4**, 493 (1994).
- [16] A. M. Tsvelik, New fermionic description of quantum spin liquid state, *Phys. Rev. Lett.* **69**, 2142 (1992).
- [17] A. M. Tsvelik, *Quantum Field Theory in Condensed Matter Physics*, 2nd ed. (Cambridge University Press, 2003).
- [18] P. Coleman, E. Miranda, and A. Tsvelik, Possible realization of odd-frequency pairing in heavy fermion compounds, *Phys. Rev. Lett.* **70**, 2960 (1993).
- [19] M. G. Ivanov, Binary representation of coordinate and momentum in quantum mechanics, *Theoretical and Mathematical Physics* **196**, 10177 (2018).
- [20] M. G. Ivanov and A. Y. Polushkin, Ternary and binary representation of coordinate and momentum in quantum mechanics, *AIP Conference Proceedings* **2362**, 040002 (2021), https://pubs.aip.org/aip/acp/article-pdf/doi/10.1063/5.0055033/14233211/040002_1_online.pdf.
- [21] M. G. Ivanov and A. Y. Polushkin, Digital representation of continuous observables in quantum mechanics, *Theoretical and Mathematical Physics* **218**, 482 (2024).
- [22] A. Einstein, B. Podolsky, and N. Rosen, Can quantum-mechanical description of physical reality be considered complete?, *Phys. Rev.* **47**, 777 (1935).
- [23] A. Aspect, P. Grangier, and G. Roger, Experimental realization of einstein-podolsky-rosen-bohm gedankenexperiment: A new violation of bell's inequalities, *Phys. Rev. Lett.* **49**, 91 (1982).
- [24] R. Moessner and J. E. Moore, *Topological Phases of Matter* (Cambridge University Press, 2021) p. i-iv.
- [25] J. Schliemann, J. a. V. I. Costa, P. Wenk, and J. C. Egues, Many-body localization: Transitions in spin models, *Phys. Rev. B* **103**, 174203 (2021).
- [26] J. Siegl and J. Schliemann, Imperfect many-body localization in exchange-disordered isotropic spin chains, *New Journal of Physics* **25**, 123002 (2023).
- [27] M. Goihl, M. Gluza, C. Krumnow, and J. Eisert, Construction of exact constants of motion and effective models for many-body localized systems, *Phys. Rev. B* **97**, 134202 (2018).
- [28] J. Parkinson and D. Farnell, *An Introduction to Quantum Spin Systems*, Lecture Notes in Physics (Springer Berlin Heidelberg, 2010).
- [29] A. W. Sandvik, Computational studies of quantum spin systems, *AIP Conference Proceedings* **1297**, 135 (2010), <https://aip.scitation.org/doi/pdf/10.1063/1.3518900>.
- [30] M. B. Kenmoe, Out-of-time ordered correlator in a fragmented hilbert space, In preparation (2024).
- [31] N. J. Jung, JH., Guide to exact diagonalization study of quantum thermalization, *J. Korean Phys. Soc.* **76**, 670 (2020).
- [32] When S_j^- acts upon the state $|n\rangle$ and meets $\sigma_n^{(j)} = 1$ at the j th position, it returns 0. When in contrary it encounters $\sigma_n^{(j)} = 0$, then it returns 1 and flip the corresponding bit leading to the state $|\mu_j^{[n]}\rangle$ with $\mu_j^{[n]} = \text{flip}(n, j)$, () .
- [33] J. J. Sakurai and J. Napolitano, *Modern Quantum Mechanics*, 2nd ed. (Cambridge University Press, 2017).
- [34] A second pair of representation can be achieved by using the conjugation relations $s_{n-q_j}^{(j)-} = s_n^{(j)+}$ and $s_{n+q_j}^{(j)+} = s_n^{(j)-}$ (see appendix B). For instance, $\hat{S}_j^+ = \sum_{n=0}^{D-1} s_n^{(j)+} |n-q_j\rangle\langle n|$ and $\hat{S}_j^- = \sum_{n=0}^{D-1} s_n^{(j)+} |n\rangle\langle n-q_j|$ supplemented by eq.(??), () .
- [35] W. Zhang and Y. Zhou, Chapter 2 - level-set functions and parametric functions, in *The Feature-Driven Method for Structural Optimization*, edited by Z. Weihong and Z. Ying (Elsevier, 2021) pp. 9–46.
- [36] V. John, An analytic exact form of the unit step function, *Mathematics and Statistics* **2**, 235 (2014).
- [37] Indeed, if q and r respectively denote the quotient and the remainder of an integer a divided by b then, $r = a - bq$, () .
- [38] L. Landau, E. Lifshitz, and L. Pitaevskii, *Statistical Physics: Theory of the Condensed State*, Course of theoretical physics (Elsevier Science, 1980).
- [39] H. Bethe, Zur theorie der metalle, *Zeitschrift für Physik* **71**, 10.1007/BF01341708 (1931).
- [40] D.-g. Zhang, L. Cheng, and B.-z. Li, Algebraic bethe ansatz for the heisenberg model with the dzyaloshinsky-moriya interaction and the growth model, *Phys. Rev. B* **59**, 8379 (1999).
- [41] D. Hetterich, N. Y. Yao, M. Serbyn, F. Pollmann, and B. Trauzettel, Detection and characterization of many-body localization in central spin models, *Phys. Rev. B* **98**, 161122 (2018).
- [42] Y. Li, P. Sala, and F. Pollmann, Hilbert space fragmentation in open quantum systems, *Phys. Rev. Res.* **5**, 043239 (2023).
- [43] M. Ganguli, S. Aditya, and D. Sen, Aspects of hilbert space fragmentation in the quantum east model: Fragmentation, subspace-restricted quantum scars, and effects of density-density interactions, *Phys. Rev. B* **111**, 045411 (2025).
- [44] H. Barentzen, An analytic study of the Exe Jahn-Teller polaron, *The European Physical Journal B - Condensed Matter and Complex Systems* **24**, 10.1007/s100510170007 (2001).
- [45] E. Ising, Beitrag zur theorie des ferromagnetismus, *Zeitschrift für Physik* **31**, 10.1007/BF02980577 (1925).
- [46] W. N. Yessen, Properties of 1d classical and quantum ising models: Rigorous results, *Annales Henri Poincaré* **15**, 10.1007/s00023-013-0252-x (2014).
- [47] P. W. Anderson, Absence of diffusion in certain random lattices, *Phys. Rev.* **109**, 1492 (1958).
- [48] A brief introduction to anderson localization, .
- [49] D. Jiles, *Introduction to Magnetism and Magnetic Materials, Second Edition* (Taylor & Francis, 1998).
- [50] S. Sachdev, *Quantum Phase Transitions* (Cambridge University Press, 2011).
- [51] H. Nishimori, *Statistical Physics of Spin Glasses and Information Processing: An Introduction*, International series of monographs on physics (Oxford University Press, 2001).
- [52] H. Stanley, *Introduction to Phase Transitions and Criti-*

- cal Phenomena*, International series of monographs on physics (Oxford University Press, 1987).
- [53] A. S. T. Pires, The heisenberg model, in *Theoretical Tools for Spin Models in Magnetic Systems*, 2053-2563 (IOP Publishing, 2021) pp. 1–1 to 1–16.
- [54] T. J. Osborne, Statics and dynamics of quantum xy and heisenberg systems on graphs, *Phys. Rev. B* **74**, 094411 (2006).
- [55] K. Yokomizo and S. Murakami, Non-bloch band theory of non-hermitian systems, *Phys. Rev. Lett.* **123**, 066404 (2019).
- [56] J. Stolze and V. S. Viswanath, Dynamics of semi-infinite quantum spin chains at $T = \infty$, (2018).
- [57] F. Benatti, R. Floreanini, and L. Memarzadeh, Exact steady state of the open xx -spin chain: Entanglement and transport properties, *PRX Quantum* **2**, 030344 (2021).
- [58] .
- [59] K. S. Tikhonov and A. D. Mirlin, Many-body localization transition with power-law interactions: Statistics of eigenstates, *Phys. Rev. B* **97**, 214205 (2018).
- [60] D. Vu, K. Huang, X. Li, and S. Das Sarma, Fermionic many-body localization for random and quasiperiodic systems in the presence of short- and long-range inter-
- actions, *Phys. Rev. Lett.* **128**, 146601 (2022).
- [61] C. X. Yu, L.-A. Wu, and D. Segal, Theory of quantum energy transfer in spin chains: Superechange and ballistic motion, *The Journal of Chemical Physics* **135**, 234508 (2011), https://pubs.aip.org/aip/jcp/article-pdf/doi/10.1063/1.3668083/15446649/234508_1_online.pdf.
- [62] B. P. Lanyon, T. J. Weinhold, N. K. Langford, J. L. O'Brien, K. J. Resch, A. Gilchrist, and A. G. White, Manipulating biphotonic qutrits, *Phys. Rev. Lett.* **100**, 060504 (2008).
- [63] F. Dolde, V. Bergholm, Y. Wang, I. Jakobi, B. Naydenov, S. Pezzagna, J. Meijer, F. Jelezko, P. Neumann, T. Schulte-Herbrüggen, J. Biamonte, and J. Wrachtrup, High-fidelity spin entanglement using optimal control, *Nature Communications* **5**, 3371 (2014).
- [64] M. Kenmoe, R. Kriemann, M. Smerlak, and A. S. Zadorin, A fast iterative algorithm for near-diagonal eigenvalue problems, *SIAM Journal on Matrix Analysis and Applications* **43**, 1573 (2022), <https://doi.org/10.1137/21M1401474>.
- [65] M. Günther and L. Klotz, Schur's theorem for a block hadamard product, *Linear Algebra and its Applications* **437**, 948 (2012).